Structure and Phase Behavior of Lipid Suspensions Containing Phospholipids with Covalently Attached Poly(ethylene glycol)

A. K. Kenworthy,* S. A. Simon,‡ and T. J. McIntosh*
*Department of Cell Biology and ‡Departments of Neurobiology and Anesthesiology, Duke University Medical Center, Durham, North Carolina 27710 USA

ABSTRACT Liposomes containing phospholipids with covalently attached poly(ethylene glycol) (PEG-lipids) are being developed for in vivo drug delivery. In this paper we determine the structure and phase behavior of fully hydrated distearoylphosphatidylcholine (DSPC) suspensions containing PEG-lipids composed of distearoylphosphatidylethanolamine with attached PEGs of molecular weights ranging from 350 to 5000. For DSPC:PEG-lipid suspensions containing 0–60 mol % PEG-lipid, differential scanning calorimetry shows main endothermic transitions ranging from 55 to 64°C, depending on the size of the PEG and concentration of PEG-lipid. The enthalpy of this main transition remains constant for all PEG-350 concentrations but decreases with increasing amounts of PEG-750, PEG-2000, or PEG-5000, ultimately disappearing at PEG-lipid concentrations greater than about 60 mol %. Low-angle and wide-angle x-ray diffraction show that tilted gel ($L\beta'$) phase bilayers are formed for all PEG-lipid molecular weights at concentrations of about 10 mol % or less, with the distance between bilayers depending on PEG molecular weight and PEG-lipid concentration. At PEG-lipid concentrations greater than 10 mol %, the lipid structure depends on the size of the PEG moiety. X-ray diffraction analysis shows that untilted interdigitated ($L\beta I$) gel phase bilayers form with the incorporation of 40–100 mol % PEG-350 or 20–70 mol % PEG-750, and untilted gel ($L\beta$) phase bilayers are formed in the presence of about 20–60 mol % PEG-2000 and PEG-5000. Light microscopy, turbidity measurements, x-ray diffraction, and ^{1}H-NMR indicate that a pure micellar phase forms in the presence of greater than about 60% PEG-750, PEG-2000, or PEG-5000.

INTRODUCTION

The use of liposomes for in vivo drug delivery has been a longstanding goal of many researchers and clinicians. Until recently this goal has proven elusive, mainly because conventional liposomes injected into the bloodstream are quickly taken up by macrophages primarily located in the liver or spleen and therefore cannot be effectively targeted to other locations in the body. However, in the last few years important advances have been made in liposome design. Specifically, the incorporation into liposomes of phospholipids with poly(ethylene glycol) (PEG) chains covalently attached to their polar head group has been shown to markedly increase their time in the blood circulation (Klibanov et al., 1990; Blume and Cevc, 1990; Allen et al., 1991; Papahadjopoulos et al., 1991; Klibanov and Huang, 1992). Due to the increased circulation time of these PEG-liposomes and the leakiness of the microcirculation in solid tumors, PEG-liposomes containing anticancer drugs have been shown to accumulate preferentially in tumors (Torchilin et al., 1992; Ahmad et al., 1993; Allen et al., 1994; Blume et al., 1993; Wu et al., 1993). Moreover, recent studies have shown that drugs delivered to solid tumors with PEG-liposomes are effective in arresting tumor growth or even in decreasing the size of the tumor (Mayhew et al., 1992; Vaage et al., 1993; Williams et al., 1993).

The increased circulation time of liposomes containing PEG-lipids has been attributed to the steric repulsive barrier around the liposome provided by the covalently attached PEG (Lasic et al., 1991a; Needham and McIntosh, 1991; Papahadjopoulos et al., 1991; Needham et al., 1992; Woodle and Lasic, 1992; Blume and Cevc, 1993). In a similar manner, attached polymers have often been used to stabilize colloidal dispersions (Napper, 1983), and polymers grafted onto the surfaces of implanted medical devices prevent their fouling by adsorbed plasma proteins (Lee et al., 1989; Bridgett et al., 1992; Desai et al., 1992). Due in part to the practical importance of grafted polymers, several theoretical (Dolan and Edwards, 1974; Alexander, 1977; Klein and Luckham, 1984; Milner, 1988; deGennes, 1988; Milner et al., 1988; Patel et al., 1988; Jeon et al., 1991; Milner, 1991; Hristova and Needham, 1994) and experimental (Israelachvili et al., 1979; Klein and Luckham, 1982, 1984; Klein and Pincus, 1982; Luckham and Klein, 1985; Claesson and Gölander, 1987; Tirrell et al., 1987; Marra and Hair, 1988; Patel and Tirrell, 1989; Costello et al., 1993) analyses have been performed to determine the range and magnitude of the steric barrier produced by attached polymers. Although most of these theoretical treatments considered very long terminally attached polymers, a recent Monte Carlo simulation suggests that polymer scaling treatments are applicable for PEG chains containing as few as 10 mers (Sarmoria and Blankschtein, 1992). Two key parameters in the theoretical analyses of the interactions between surfaces with adsorbed polymers (Alexander, 1977; deGennes, 1988; Milner, 1991) are

Received for publication 17 October 1994 and in final form 9 February 1995.

Address reprint requests to Dr. Thomas J. McIntosh, Department of Cell Biology, Duke University Medical Center, Box 3011, Durham, NC 27710. Tel.: 919-684-8950; Fax: 919-684-3687; E-mail: tom_mcintosh@cellbio.duke.edu.

Dr. Kenworthy's present address is: Biology Department, Johns Hopkins University, 3400 N. Charles St., Baltimore, MD 21218.

0006-3495/95/05/1903/18 $2.00

the grafting density (or the distance between grafting points on the surface) and the length of the grafted polymer. Thus, experiments testing these theoretical treatments must be able to systematically vary these parameters.

Recent experimental studies have used a surface force balance (Israelachvili and Adams, 1976) to measure the interactions between 1) polymers or block copolymers adsorbed to smooth mica surfaces as a function of polymer molecular weight (Israelachvili et al., 1979; Klein and Luckham, 1982, 1984; Klein and Pincus, 1982; Luckham and Klein, 1985; Claesson and Gölander, 1987; Tirrell et al., 1987; Marra and Hair, 1988; Patel and Tirrell, 1989; Taunton et al., 1990; Costello et al., 1993) and 2) lipid bilayers containing one particular PEG-lipid (PEG-2000) deposited onto mica surfaces (Kuhl et al., 1994). These studies have provided important information on the range and magnitude of the steric barrier provided by adsorbed or grafted polymers. However, the results of such studies cannot necessarily be extended to the PEG-liposome systems because the formation of a steric barrier in the PEG-liposomes depends on the ability of the lipids to self-associate to form stable bilayers, and it is not known how different concentrations of PEG-lipid with various PEG molecular weights modify the bilayer structure. That PEG-lipid/phospholipid mixtures do not form bilayers at all concentrations was demonstrated by Lasic et al. (1991), who found that PEG-2000 converts liquid crystalline bilayers to micelles at concentrations greater than about 60 mol % PEG-lipid.

A second method for measuring repulsive pressures as a function of distance is by x-ray diffraction analysis of multiwalled liposomes subjected to known osmotic stress (Le-Neveu et al., 1977; Parsegian et al., 1979, 1986; McIntosh and Simon, 1986). Therefore multiwalled liposomes containing various concentrations of PEG-lipids have the potential to provide another system to measure steric repulsive pressures caused by surface-grafted polymers, to test theories for steric pressures for the case of relatively small grafted polymers, and to provide direct information on the magnitude and range of the steric barrier produced by the incorporation of PEG-lipids in liposomes. Such x-ray diffraction/osmotic stress studies have been performed for a single PEG-lipid concentration and molecular weight (PEG-2000) (Needham et al., 1992). However, as a prelude to extending such osmotic stress experiments, it must be shown that relatively wide ranges of both concentration of PEG-lipids and size of attached PEG can be incorporated into the liposomes without appreciably modifying the bilayer structure.

In this study we use a variety of techniques, including differential scanning calorimetry, x-ray diffraction, nuclear magnetic resonance (NMR), light microscopy, and turbidity measurements, to determine 1) the effect of a PEG-lipid on gel-phase bilayer structure, 2) the maximum amount of PEG-lipid that can be incorporated into gel-phase bilayers, and 3) phase diagrams of phospholipid/PEG-lipid suspensions. We focus on PEG-lipids containing four different polymer molecular weights, 350, 750, 2000, and 5000. These particular PEG-lipids, with the PEG covalently attached to distearoylphosphatidylethanolamine (DSPE), have previously been used in studies to determine the effects of polymer lipids on the circulation time of liposomes (Allen et al., 1991; Lasic et al., 1991a; Papahadjopoulos et al., 1991). In our analysis, we use distearoylphosphatidylcholine (DSPC) as the host lipid in the liposomes, since DSPC has the same chain composition as the PEG-lipids and since the structure and thermal properties of DSPC liposomes are well understood (Mabrey and Sturtevant, 1976; Janiak et al., 1979). Moreover, it has been found that the blood circulation times for DSPC:PEG-liposomes are similar to those of other PEG-liposomes (Woodle and Lasic, 1992).

In this first paper we present the structure and phase diagram of dispersions of DSPC:PEG-lipids and in the accompanying paper (Kenworthy et al., 1995) we present complete pressure-distance isotherms for DSPC:PEG-lipid mixtures over PEG-lipid concentration ranges where bilayers are formed.

MATERIALS AND METHODS

Materials

DSPC was obtained from Avanti Polar Lipids (Alabaster, AL). The PEG-lipids consisted of distearoylphosphatidylethanolamine with various molecular weights of poly(ethylene glycol) (PEG) covalently attached to the amine group (*N*-(carbamyl-polyethylene glycol) methyl ether)-1,2-distearoyl-*sn*-glycerol-3-phosphoethanolamine). The PEG-lipids used in these studies contained PEGs with average molecular weights of 350, 750, 2000, and 5000, and are subsequently referred to as PEG-350, PEG-750, PEG-2000, and PEG-5000, respectively. PEG-lipids were obtained from two sources. For most experiments, the lipids were a gift from Liposome Technology, Inc. These lipids have been used in a number of in vivo drug delivery studies (Allen et al., 1991; Lasic et al., 1991; Papahadjopoulos et al., 1991; Wu et al., 1993). The purity of these PEG-lipids was stated to be about 98%. For some experiments (where indicated), high purity (>98%) PEG-lipids with PEG molecular weights of 2000 and 5000 were obtained from Avanti Polar Lipids (Alabaster, AL). These lipids are referred to as Avanti PEG-2000 and Avanti PEG-5000, respectively. Both the Liposome Technology and Avanti PEG-lipids contained covalently attached PEGs made by Union Carbide (South Charleston, WV). As kindly provided by Union Carbide, typical values for the weight-average molecular weight (M_w) and the number-average molecular weight (M_n) for PEG chains used in the synthesis of PEG-lipids were: PEG 750, M_w = 739, M_n = 670; PEG 2000, M_w = 2211, M_n = 2059; and PEG 5000, M_w = 5581, M_n = 5394.

The amount of water in typical PEG-lipid samples was determined by comparing the weight of the samples before and after vacuum dessication for 12 to 36 h over phosphorous pentoxide. The measured wt % water contents were 5.6% for PEG-750, 0.2% for PEG-2000, and 2.0% for PEG-5000.

Dextran with an average molecular weight of 503,000 Da and poly-(vinylpyrrolidone) (PVP) with an average molecular weight of 40,000 Da were purchased from Sigma Chemical Co. (St. Louis, MO.). Polyethylene glycol with number-average molecular weights of 1420 and 3336 Da were obtained from Scientific Polymer Products (Ontario, NY). Deuterium oxide (99.9%) was obtained from Cambridge Isotope Laboratories (Woburn, MA) and 3-(trimethylsilyl)-1-propanesulfonic acid (DSS) was obtained from Aldrich (Milwaukee, WI).

Sample preparation

Mixtures of DSPC and PEG-lipids were co-dissolved in chloroform. After removal of the chloroform by rotary evaporation, excess amounts (>90% by weight) of buffer (100 mM NaCl, 20 mM HEPES in H_2O, pH 7.0 for most

experiments and in D_2O, pD 7.0 for NMR experiments) were added to the dry lipid. HEPES was chosen as the buffer because it has a relatively small change in pK_a with respect to temperature. To obtain complete hydration, the lipid suspensions were incubated at 70°C (above the main phase transition temperature of both DSPC and the PEG-lipids), periodically vortexed, and cycled through the main phase transition temperature at least three times. For some x-ray diffraction experiments, dextran or PVP were added to the buffer to apply an osmotic pressure to the liposomes to improve the orderliness of the bilayer stacking and thereby improve the diffraction pattern (McIntosh and Simon, 1986). Osmotic pressures of dextran and PVP solutions as a function of polymer concentration have previously been measured (Parsegian et al., 1986; McIntosh et al., 1989b).

Light microscopy

For light microscopy, a small drop of specimen was placed on clean glass slide, gently covered with a thin glass coverslip, and placed on the stage of a Zeiss microscope. Specimens were observed with bright field illumination and with phase contrast. Birefringence studies were made with the addition of crossed nicol filters (polarizer and analyzer) (Bourges et al., 1967).

Absorbance measurements

Absorbance measurements were made for suspensions with a DSPC concentration of 1 mM with a Beckman Model 25 spectrophotometer using a wavelength of 520 nm. To avoid foaming, specimens for the absorbance measurements were shaken by hand.

Differential scanning calorimetry

For calorimetry, dry DSPC:PEG-lipid samples (1–6 mg each) were placed into the sample pans, 90% by weight buffer (100 mM NaCl, 20 mM HEPES, pH 7.0); or unbuffered 100 mM NaCl was added, the sample pans were hermetically sealed and incubated in an oven at 70°C. Thermograms were recorded using a Perkin-Elmer Differential Scanning Calorimeter (DSC-7) at a heating rate of 5°C/min. With this sample preparation technique, successive calorimetric heating scans gave identical results. The transition temperature (T_m) was measured as the temperature at the peak of the endothermic transition. Enthalpies were obtained using software provided by Perkin-Elmer that gives the areas under the heat capacity peaks. Where overlapping multiple peaks were observed, the transition temperature and enthalpy were estimated by fitting each peak to a Gaussian distribution.

X-ray diffraction

For x-ray diffraction, the lipid dispersions were concentrated by centrifugation with a bench centrifuge, sealed in quartz capillary tubes, and mounted in either a point collimation x-ray camera or a mirror-mirror x-ray camera. X-ray diffraction patterns were recorded at 20°C on a stack of 3–5 Kodak DEF x-ray films (Eastman Kodak, Rochester, NY) loaded in a flat plate film cassette with exposure times of 3–36 h. X-ray films were processed by standard techniques and densitometered with a Joyce-Loebl microdensitometer as described previously (McIntosh and Simon, 1986; McIntosh et al., 1987, 1989a, 1989b, 1992). After background subtraction, integrated intensities, $I(h)$, were obtained for each order h by measuring the area under each diffraction peak. The structure amplitude $F(h)$ was set equal to $\{h^2I(h)\}^{1/2}$ (Blaurock and Worthington, 1966; Herbette et al., 1977). Electron density profiles, $\rho(x)$, on a relative electron density scale were calculated from

$$\rho(x) = (2/d)\sum \exp\{i\phi(h)\}\cdot F(h)\cdot\cos(2\pi x h/d) \quad (1)$$

where x is the distance from the center of the bilayer, d is the lamellar repeat period, $\phi(h)$ is the phase angle for order h, and the sum is over h. Phase angles were determined by the use of the sampling theorem (Shannon, 1949) as described in detail previously (McIntosh and Simon, 1986; McIntosh and Holloway, 1987). Electron density profiles described in this paper are at a resolution of $d/2h_{max} \approx 8$ Å.

NMR

^1H Fourier transform NMR experiments were performed at the Duke University NMR Spectroscopy Center on a 500 MHz Varian spectrometer using a 5 mm ^1H probe at 28 and 70°C. Samples were locked and shimmed on the water line before data collection. ^1H spectra were obtained using a 6 μs 180° pulse with a delay of 20 ms, collected for up to 32 cycles, over a sweep window of 6 kHz. ^1H chemical shifts were normalized against the water resonance, which was determined in control experiments at 28 and 70°C for buffer containing an internal DSS standard.

RESULTS

Light microscopy

Light microscopy was used to determine whether an excess fluid phase was present in specimens used for x-ray diffraction analysis and also to assess the phase (bilayer or micellar) of selected DSPC:PEG-lipid specimens both above and below the transition temperature. At 20°C, 85:15 DSPC:PEG-2000 suspensions in solutions of 1%, 5%, and 15% dextran all showed by phase contrast microscopy spherical particles surrounded by excess solution. These spherical particles were birefringent when observed between crossed polarized filters, with a Maltese cross appearance typical of multilamellar vesicles (MLVs) (Bourges et al., 1967). At 20°C, samples containing 80:20 and 70:30 DSPC:PEG-2000 specimens were only slightly birefringent, and 60:40 DSPC:PEG-2000 and fully hydrated PEG-2000 were non-birefringent. Similar behavior was observed for specimens of DSPC:PEG-750 and DSPC-PEG-5000, in that at 20°C specimens containing 20 mol % or less PEG-lipid were birefringent, whereas the specimens became less and less birefringent as the concentration of PEG-lipid was progressively increased. These non-birefringent samples flowed easily when the coverslip was slightly depressed, meaning that they were either composed of micelles or small unilamellar vesicles (SUVs), rather than the comparatively viscous cubic phase.

When the samples containing ≤20 mol % PEG-lipid were heated above 65°C (above the bilayer phase transition; see below), the spherical MLVs retained their birefringence but became more deformable when the coverslip was depressed, consistent with MLVs in the liquid crystalline phase. This deformability change was reversible, as the birefringent spheres became significantly less deformable as they were cooled below 50°C.

Absorbance

Fig. 1 shows the absorbance at 520 nm for DSPC:PEG-lipid mixtures measured as a function of both PEG molecular weight and mol % PEG-lipid. For all the DSPC:PEG-lipid dispersions, the turbidity showed an initial sharp drop with addition of the lowest concentration of PEG-lipid. For PEG-750, PEG-2000, and PEG-5000, the absorbance of the solutions was similar for 1.5–10 mol % PEG-lipid, but decreased with increasing PEG-lipid concentration above 10

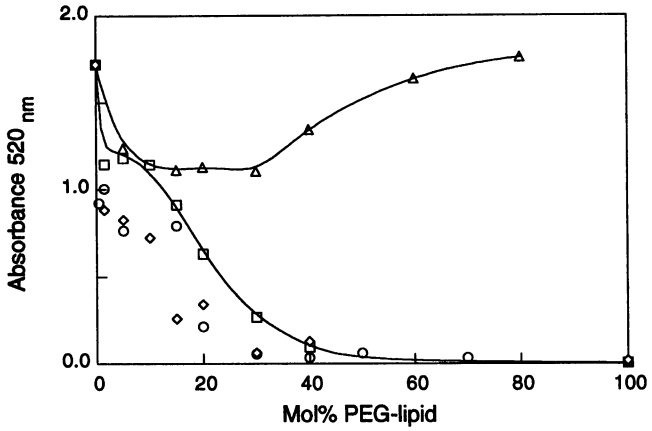

FIGURE 1 Absorbance at 520 nm for DSPC:PEG-lipid dispersions containing 1 mM DSPC as a function of mol % PEG-lipid for PEG-350 (△), PEG-750 (□), PEG-2000 (○), and PEG-5000 (◇). The lines through the data points for PEG-350 and PEG-750 are drawn to guide the eye. The absorbance for a 1 mM PEG-350 solution is 0.233.

mol %, dropping to close to 0 at 30–40% mol % PEG-lipid. 1 mM solutions of polyethylene glycol with a number-average molecular weight of either 1420 or 3336 Da also had an absorbance of near 0 (data not shown). In contrast, for DSPC:PEG-350 suspensions, the absorbance increased gradually with increasing PEG-350 concentration (Fig. 1).

The large absorbances observed for the DSPC:PEG-lipid suspensions for PEG-lipid concentrations of 0–10 mol % (Fig. 1) are consistent with the presence of MLVs which, because of their relatively large size, scatter significantly at this wavelength (Carmona-Riberio and Chaimovich, 1986; Almog et al., 1990; Walter et al., 1991). The decrease in absorbance observed upon addition of the lowest PEG-lipid concentrations likely results from a decrease in vesicle diameter, which has been observed for egg phosphatidylcholine:PEG-2000 suspensions by light microscopy and light scattering methods (Lasic et al., 1991). The strong absorbance for the DSPC:PEG-350 samples across the entire PEG-350 concentration range suggests that MLVs were present at all DSPC:PEG-350 concentrations and implies that PEG-350 had comparatively little effect on either the mass or number of DSPC:PEG-lipid particles. The marked decrease in absorbance for suspensions containing greater than 10 mol % PEG-750, PEG-2000, and PEG-5000 indicates that the anhydrous mass of each particle was decreasing faster than the number of particles was increasing. This implies that at these PEG-lipid concentrations some of the lipid was present in a structural form that scatters light relatively weakly, such as SUVs or micelles.

Calorimetry

Fig. 2 shows selected calorimetric traces for DSPC:PEG-lipid suspensions and Fig. 3 shows the enthalpies obtained as a function of PEG-lipid concentration. In the absence of PEG-lipid, DSPC suspensions exhibited a sharp main transition at 54.5°C with an enthalpy of 55.2 J/g (10.4 Kcal/mol) and a small pretransition event at 52.0°C with an enthalpy of 5.1 J/g (1.0 Kcal/mol). These values are in good agreement with previous measurements (Hinz and Sturtevant, 1972; Mabrey and Sturtevant, 1976; Mason et al., 1981).

The thermograms (Fig. 2, *A–F*) and enthalpies (Fig. 3) of the DSPC:PEG-lipid suspensions show the following features. First, the main endothermic transition temperature was not markedly changed from its control value at approximately 55°C by the incorporation of up to 100 mol % PEG-350 (Fig. 2 *A*), 50 mol % PEG-750 (Fig. 2 *B*), 50 mol % PEG-2000 (Fig. 2 *C*), 5 mol % PEG-5000 (Fig. 2 *D*), 5 mol % Avanti PEG-2000 (Fig. 2 *E*), or 5 mol % Avanti PEG-5000 (Fig. 2 *F*). However, incorporation of >10 mol % PEG-5000, Avanti PEG-2000 or Avanti PEG-5000 increased the transition temperature by up to 10°C. Second, although the width of the main transition remained approximately constant for

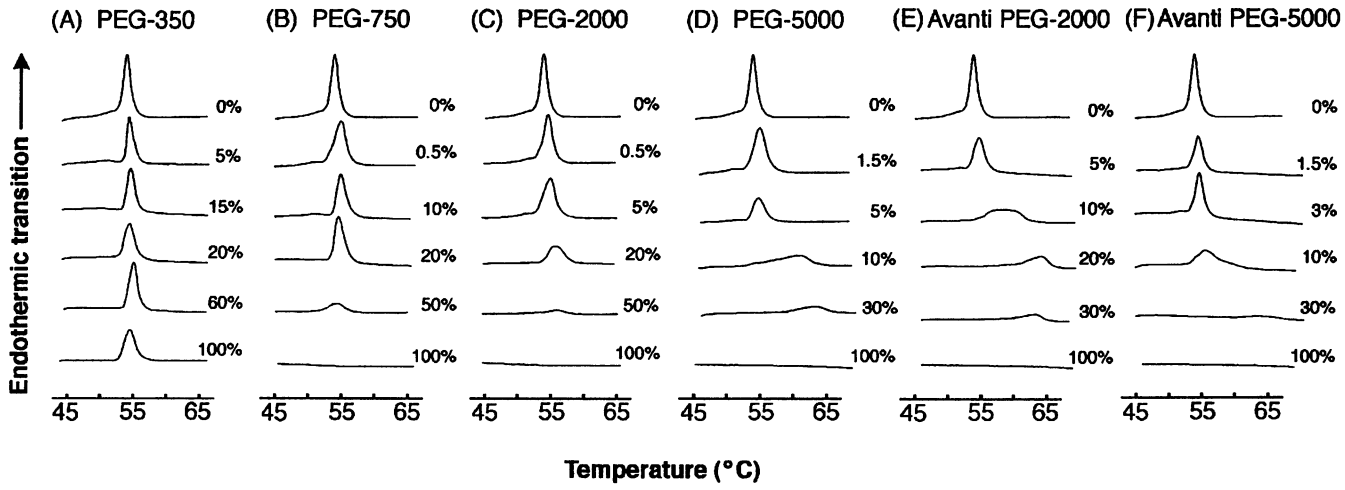

FIGURE 2 Representative calorimetric traces for DSPC:PEG-lipid dispersions containing (*A*) PEG-350, (*B*) PEG-750, (*C*) PEG-2000, (*D*) PEG-5000, (*E*) Avanti PEG-2000, and (*F*) Avanti PEG-5000. Note that all samples did not contain the same lipid concentrations. The enthalpies for these thermograms are presented in Fig. 3.

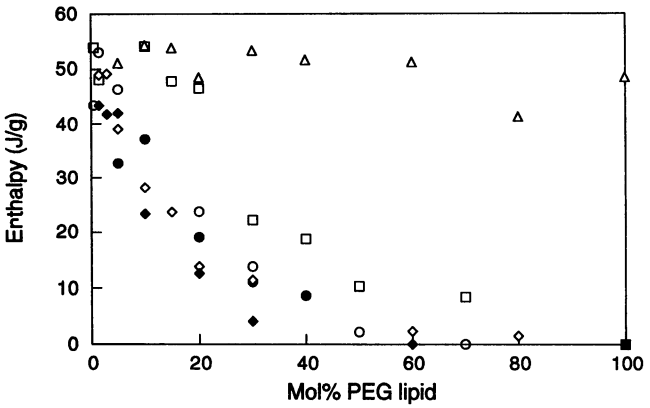

FIGURE 3 Enthalpy of the main DSPC:PEG-lipid dispersion melting transition as a function of mol % PEG-lipid for PEG-350 (△), PEG-750 (□), PEG-2000 (○), and PEG-5000 (◇), Avanti PEG-2000 (●), and Avanti PEG-5000 (◆). Enthalpy is given in J/g total lipid in the sample.

all concentrations of PEG-350 (Fig. 2 *A*), the shape of the transition was more complex for the larger PEG-lipids. For concentrations of 10–20 mol % PEG-5000, Avanti PEG-2000, or Avanti PEG-5000 there was evidence for two endothermic transitions. For example, the scan of 10 mol % PEG-5000 (Fig. 2 *D*) showed two broad peaks centered at about 55 and 62°C. From 20 to 80 mol % PEG-5000, 20–40 mol % Avanti PEG-2000, or 20–60 mol % Avanti PEG-5000 only a single peak at about 65°C was observed. Third, the enthalpy of the transition was a function of both the concentration and molecular weight of the PEG-lipid. With the exception of PEG-350, the enthalpy of the main transition decreased to 0 with increasing PEG-lipid concentrations (Fig. 3). At 100% PEG-lipid, only PEG-350 exhibited a main endothermic transition; all other PEG lipids did not exhibit a transition between 30 and 90°C. Fourth, for all PEG-lipids, the pretransition peak temperature remained nearly constant with increasing PEG-lipid up to about 10 mol %, and disappeared at higher PEG-lipid concentrations.

X-ray diffraction

The x-ray diffraction patterns contained information both on the packing of the lipid hydrocarbon chains (contained in the wide-angle diffraction for spacings around 4 Å) and on the structure of lipid assemblies (contained in the low-angle regions for spacings from 200 to 10 Å). Both the low-angle and wide-angle x-ray diffraction patterns at 20°C depended on the concentration and type of PEG-lipid in the DSPC dispersion. We first considered suspensions in excess buffer with no applied osmotic pressure. Some samples, particularly those containing high concentrations of the larger PEG-lipids (see below), gave broad bands in the low-angle region. To record discrete low-angle reflections from these specimens, it was necessary to apply relatively small osmotic stresses (as indicated) to the specimens by incubating them in PVP or dextran solutions.

Wide-angle diffraction

In excess buffer, each suspension of DSPC:PEG-lipid containing 0–10 mol % of PEG-350, PEG-750, PEG-2000, or 0–5 mol % PEG-5000 gave a wide-angle pattern with a sharp reflection at 4.22 Å and a broader band centered at 4.0 Å (Table 1). These wide-angle patterns were similar to those previously observed for gel phase ($L\beta'$) phosphatidylcholine bilayers with tilted hydrocarbon chains (Tardieu et al., 1973; McIntosh, 1980). However, the wide-angle diffraction differed for each PEG molecular weight at higher PEG-lipid concentrations as shown in Table 1. (Similar wide-angle patterns were recorded in excess buffer or in PVP or dextran solutions corresponding to osmotic pressures less than 3.6×10^5 dyn/cm^2, although the signal-to-noise ratio was generally better with the applied osmotic pressure.) The following features were observed. First, sharp wide-angle reflections were obtained for all concentrations of PEG-350, but only for PEG-lipid concentrations up to about 50% for PEG-750, PEG-2000, and PEG-5000. Second, for all PEG-lipids the

TABLE 1 Wide-angle reflections of DPSC:PEG-lipid dispersions*

Mol % PEG-lipid	PEG-350	PEG-750	PEG-2000	PEG-5000
0–3	4.22vs, 4.0b	4.22vs, 4.0b	4.22vs, 4.0b	4.22vs, 4.0b (4.22vs, 4.0b)
5	4.22vs, 4.0b	4.22vs, 4.0b	4.22vs, 4.0b (4.22s, 4.05s)	4.22vs, 4.0b (4.22s, 4.05s)
10	4.22vs, 4.0b	4.22vs, 4.0b	4.22vs, 4.0b (4.07s)	4.22vs, 4.05s (4.1b)
15	4.22vs, 4.0b	4.22vs, 4.05s	4.22vs, 4.05s	
20	4.22s, 4.05s	4.22vs, 4.05s	4.22s, 4.05s (4.07s)	4.07s
30	4.22s, 4.05s	4.05s	4.1b (4.07s)	(4.07s)
40	4.22s, 4.05s	4.05s	4.1b (4.07s)	
50		4.1b	4.1b	
60	4.05vs			
80	4.05vs			
100	4.05s	ND	ND	ND

*Wide-angle reflections are designated as very sharp (vs), sharp (s), broad (b), or not detected (ND). For specimens giving two sharp reflections, the reflection giving the stronger intensity is underlined; if sharp reflections were of approximately equal intensity, both are underlined. Data from the Avanti PEG-lipids are given in parentheses.

double wide-angle reflection (4.22 Å sharp, 4.0 Å broad) observed at low PEG-lipid concentrations was converted to a doublet of sharp reflections (4.22 and 4.05 Å) at intermediate PEG-lipid concentrations, and finally to a single sharp reflection (at either 4.05 or 4.07 Å) at high concentrations of PEG-lipid. The concentrations at which these sharp double and single reflections were observed depended on the size of the PEG-lipid (Table 1). In the concentration ranges where the double sharp wide angle reflections were observed, the relative intensity of the 4.05 Å reflection to the 4.22 Å reflection increased with increasing PEG-lipid concentration until eventually the 4.22 Å reflection was not observed (Table 1). Third, for some samples a relatively broad reflection centered near 4.1 Å was observed (Table 1). It could not be determined whether this broad band was comprised of a single broad reflection or two overlapping reflections.

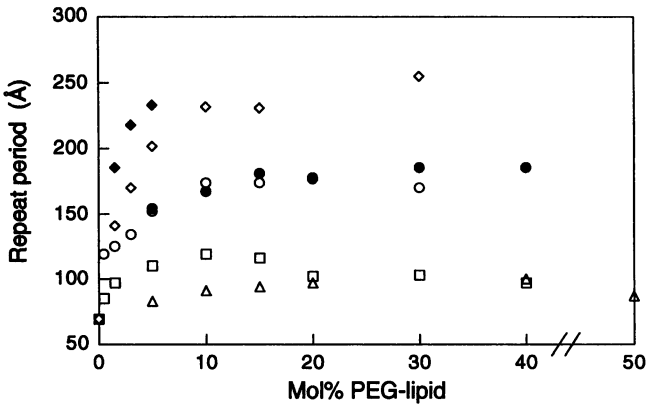

FIGURE 4 Lamellar repeat period for DSPC:PEG-lipid dispersions at an applied pressure of 1×10^5 dyn/cm^2 as a function of mol % PEG-lipid for PEG-350 (△), PEG-750 (□), PEG-2000 (○), and PEG-5000 (◇), Avanti PEG-2000 (●), and Avanti PEG-5000 (◆).

Low-angle diffraction data

In excess buffer with no applied pressure, discrete low-angle reflections were obtained for DSPC:PEG-lipid specimens containing 0–100 mol % PEG-350, 0–5 mol % PEG-750, or 0–3 mol % PEG-2000. Depending on the concentration and molecular weight of the PEG-lipid, the observed lamellar repeat periods ranged from about 70 to 170 Å. For higher concentrations of PEG-750, PEG-2000, or any concentration of PEG-5000, the low-angle diffraction in excess buffer contained broad diffraction bands. For the 3–60 mol % DSPC:PEG-2000 or the 1.5–60 mol % DSPC:PEG-5000 specimens these bands were centered at 0.022 Å^{-1} and 0.042 Å^{-1}, which are at reciprocal spacings similar to those observed for the first two peaks in continuous transforms of gel phase phosphatidylcholine bilayers (McIntosh and Simon, 1986). These patterns imply that the sample contained either single walled vesicles or else multiwalled vesicles with large and nonuniform fluid spaces between adjacent bilayers. To obtain discrete low-angle reflections from these specimens it was necessary to improve the lamellar stacking by applying an osmotic pressure.

When osmotic pressures in the range of 8.9×10^2 to 1.7×10^7 dyn/cm^2 were applied to the DSPC:PEG-lipid suspensions, low-angle lamellar repeat periods were observed that depended both on PEG-lipid concentration and PEG-lipid molecular weight. The full pressure-distance relationships obtained for these lipids are presented and analyzed in the accompanying paper (Kenworthy et al., 1995). In this paper we focus on the structure of the DSPC:PEG-lipid suspensions, particularly at relatively low applied pressures. Fig. 4 shows the lamellar repeat periods of DSPC:PEG-lipid samples for PEG-350, PEG-750, PEG-2000, and PEG-5000 plotted as a function of mol % PEG-lipid at an applied pressure of 1.0×10^5 dyn/cm^2. For each of these PEG-lipids the repeat period increased with increasing PEG-lipid concentration up to about 10 mol % PEG-lipid. The repeat periods for DSPC suspensions containing PEG-2000 and PEG-5000 stayed approximately constant with increasing PEG-lipid concentrations for concentrations above about 10 mol % PEG-lipid. For DSPC:PEG-2000 the repeat period versus concentration curves (Fig. 4) were similar for the Avanti and Liposome Tech preparations. However, for DSPC:PEG-5000 the repeat period versus concentration curve was shifted to the left for the Avanti lipid compared with the Liposome Tech preparation (Fig. 4), i.e., the repeat period reached its maximum value with smaller nominal concentrations of Avanti PEG-5000 than Liposome Technology PEG-5000. Possible sources of this observed difference in results from the Avanti and Liposome Tech PEG-5000 preparations could be errors in the gravimetric measurements due to differences in either 1) lipid purity, 2) water content of the PEG-lipid powder, or 3) PEG molecular weight polydispersity. We have not pursued this point further.

An interesting feature of the DSPC:PEG-750 suspensions was that as the PEG-750 concentration was increased from 15 to 20 mol % there was a 15 Å decrease in repeat period. A similar phenomenon occurred for DSPC:PEG-350 mixtures, where the repeat period decreased about 15 Å from 40 to 100 mol % PEG-350. Although PEG-350 gave lamellar diffraction out of 100 mol %, no discrete low-angle diffraction was observed for 100 mol % PEG-750, PEG-2000, or PEG-5000.

The maximum observed repeat period was a strong function of the PEG-lipid, being about 80 Å for DSPC:PEG-350, 120 Å for DSPC:PEG-750, 170 Å for DSPC:PEG-2000, and 250 Å for DSPC:PEG-5000 (Fig. 4).

Fig. 5 gives the structure factors for the low-angle reflections of DSPC and DSPC:PEG-lipid mixtures containing up to 15 mol % PEG-lipid. The repeat periods represented here ranged from 67 to 166 Å for applied pressures ranging from 1.0×10^5 to 2.3×10^7 dyn/cm^2. The solid line represents a continuous transform calculated for one of the DSPC data sets using the sampling theorem (Sayre, 1952; Worthington et al., 1973). For this calculation, the structure factor at the origin of reciprocal space, $F(0)$, was determined based on the results of strip modeling (described below). Note that the structure factors for the DSPC:PEG-lipid samples fell near

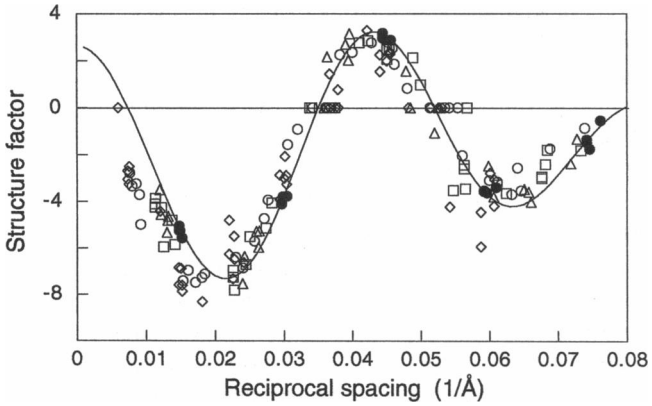

FIGURE 5 Structure factors for DSPC (●) and DSPC:PEG-lipid mixtures (*open symbols*) plotted versus reciprocal space coordinates. Data are shown for DSPC:PEG-lipid mixtures containing 0.5–15 mol % PEG-lipid for PEG-350 (△), PEG-750 (□), PEG-2000 (○), and PEG-5000 (◇), with repeat periods ranging from 71 to 166 Å for applied pressures of 1×10^5 to 2.3×10^7 dyn/cm^2. The solid line is a continuous Fourier transform calculated using the sampling theorem for one of the DSPC data sets, with $F(0) = 2.64$ based on the results of a uniform electron density strip model (as described in the text).

the DSPC transform, indicating that the phase angles for these reflections were the same as for the corresponding reflections from DSPC.

Analysis of low-angle diffraction data

Although the structure factors for DSPC:PEG-lipid samples were similar to those for DSPC bilayers (Fig. 5), there were systematic differences in particular regions of reciprocal space. For instance, the structure factors for samples containing PEG-lipid fell slightly below the continuous transform of DSPC in the region of reciprocal space from 0.007 to 0.022 Å^{-1}. To determine whether these small differences in the structure factors could be due to the covalently attached PEG increasing the density of the fluid layer between bilayers, we calculated Fourier transforms of uniform electron density strip models (Worthington, 1969) for the structures of DSPC bilayers with and without PEG-lipids. The DSPC bilayer structure was approximated by five strips of uniform electron density, one representing the terminal methyl region, two representing the acyl chain regions, and two representing the phospholipid headgroup regions. As a starting point for modeling the DSPC structure factors, we assumed electron densities of 0.27, 0.32, and 0.45 electrons/Å^3, and widths of 6.0, 15.5, and 10.0 Å for the strips corresponding to the terminal methyl, hydrocarbon, and headgroup regions, respectively. These electron densities and widths are similar to those previously determined for phosphatidylcholine bilayers (McDaniel and McIntosh, 1986; McIntosh and Holloway, 1987). So that the fluid space between adjacent bilayers did not contribute to the calculation of the transform, the density of the buffer in the fluid space, 0.336 electrons/Å^3, was subtracted from each of the strips. The strip model was then fit to the structure factor data by simultaneously modifying the width of the terminal methyl and methylene regions and electron density of the terminal methyl region. The best fit ($R = 0.964$) was obtained for values of 8.0 Å, 13.8 Å, and 0.234 electrons/Å^3 for the terminal methyl width, methylene width, and terminal methyl density, respectively. The results of these fits were used to obtain an average value of $F(0) = +2.6$ for DSPC. This value for $F(0)$ was used in the calculation of continuous transforms by the sampling theorem (Fig. 5). To model the bilayers containing the PEG-lipids, the same five-strip model was used with the same electron densities and widths as determined for DSPC. However, to account for the contribution of the covalently attached PEG, the electron density in the fluid space was allowed to vary. The results of these calculations are summarized in Fig. 6, where continuous transforms are shown for several representative data sets. These model calculations show that for a constant concentration of 5 mol % PEG-lipid in the DSPC bilayer, the electron density in the fluid space was significantly higher for PEG-750 (0.354 ± 0.007 electrons/Å^3), PEG-2000 (0.358 ± 0.002 electrons/Å^3), and PEG-5000 (0.360 ± 0.008 electrons/Å^3) than for PEG-350 (0.334 ± 0.009 electrons/Å^3). (These electron densities correspond to relatively low aqueous concentrations of PEG. For example, by estimating the volume per PEG in the fluid space from the area per lipid molecule of 48 Å^2 and the width of the fluid space determined below, we estimate that a value of 0.358 electrons/Å^3 corresponds to a 6 wt % solution of 2000 molecular weight PEG.) These model calculations show that the overall effect of this increase in electron density in the fluid space was to shift the position of the first peak in the continuous transform in a manner consistent with the experimental results (Fig. 5). Thus, the observed effect of PEG-lipid incorporation on the DSPC transform could be

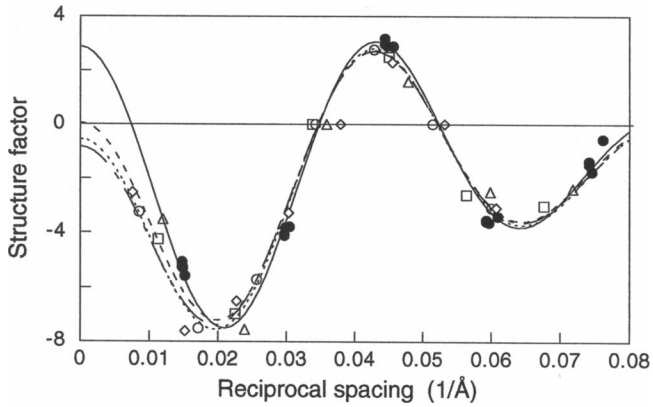

FIGURE 6 Strip models calculations demonstrating the effect of changes in fluid space electron density on DSPC:PEG-lipid structure factors (see text for details). Representative structure factor data (taken from Fig. 5) are shown for DSPC and DSPC:PEG-lipid suspensions containing 5% PEG- 350 (applied pressure = 1.0×10^5 dyn/cm^2) (△), 5% PEG-750 (applied pressure = 2.0×10^6 dyn/cm^2) (□), 5% PEG-2000 (applied pressure = 2.0×10^6 dyn/cm^2) (○), and 5% PEG-5000 (applied pressure = 4.2×10^6 dyn/cm^2) (◇). Fits of the uniform electron density strip model are shown for PEG-350 (———), PEG-750 (---), PEG-2000 (·····), and PEG-5000 (-·-·-·).

accounted for by increasing the electron density in the fluid space without significantly changing the bilayer structure.

The structure factor data in Fig. 5 were used to calculate electron density profiles for each unit cell of the multilayer. Fig. 7 shows electron density profiles for DSPC bilayers containing the different PEG-lipids at a constant PEG-lipid concentration of 15 mol % and applied pressure of about 1.5×10^7 dyn/cm^2. A single unit cell is shown for each, with the middle of the bilayer centered at 0 Å. The low density trough in the center of each bilayer corresponds to the localization of the terminal methyl groups on the lipid hydrocarbon chains, the medium density regions on both sides of the terminal methyl trough correspond to the methylene groups of the hydrocarbon chains, the high density peaks centered at ±25 Å correspond to the phospholipid head groups, and the medium density regions beyond ±35 Å correspond to half the fluid space between adjacent bilayers.

The profiles in Fig. 7 show that: 1) the width of the fluid space increased with increasing PEG molecular weight and 2) the width of the bilayer, as measured by the headgroup peak-to-peak separation, remained nearly constant with the incorporation of 15 mol % PEG-lipid. Relative to the second point, the profiles show a nearly constant headgroup peak-to-peak distance of 47.3 ± 0.4 Å (mean ± SD, $N = 24$ experiments), consistent with the gel phase ($L\beta'$) DSPC bilayer (Fig. 7, *top profile*). Thus, although there were changes in the wide-angle patterns at 15 mol % lipid (Table 1), the electron density profiles showed that the bilayer thickness was not appreciably changed. Therefore it appears that at 15 mol % PEG-lipid the bilayers are in a tilted gel phase with slightly altered hydrocarbon packing from pure DSPC bilayers. When grouped separately by PEG molecular weight, the peak-to-peak distance for DSPC bilayers containing PEG-5000 (49.0 ± 0.6 Å, $N = 6$ experiments) was somewhat larger than for those containing PEG-350, PEG-750, or PEG-2000. Two possible factors could account for this slightly larger headgroup peak-to-peak distance in DSPC:PEG-5000 bilayers: 1) PEG-5000 could cause a small increase in bilayer thickness by decreasing the hydrocarbon chain tilt, and 2) the large electron density in the fluid space caused by the PEG-5000 could shift the position of the head group peak in the electron density profiles.

Thus, the low-angle x-ray data showed that the DSPC:PEG-lipid samples with PEG-lipid concentrations of 0–15 mol % had similar bilayer structures to DSPC, despite small differences in the wide-angle reflections for these samples. In contrast, as described below, both the wide-angle and low-angle data showed that DSPC suspensions containing over 20 mol % PEG-lipids had different structures, which depended on the size of the PEG-lipid.

We first consider the structure of DSPC suspensions containing 60–100 mol % PEG-350 and 30–40 mol % PEG-750. These samples all gave a single sharp wide angle reflection at 4.05 Å (Table 1). The structure factors derived from the low-angle diffraction for these suspensions (Fig. 8) did not fall on the same transform as DSPC (Fig. 5). In particular, these specimens produced strong reflections at reciprocal space coordinates around 0.035 Å^{-1} (Fig. 8), a region where the DSPC transform passed through a zero (Fig. 5). The wide-angle reflection (Table 1) and the low-angle structure factors for these specimens were similar to those found for the interdigitated ($L\beta I$) gel phase, where the hydrocarbon chains from apposing monolayers of the lipid bilayer interpenetrate or interdigitate (McIntosh et al., 1983). Therefore, in Fig. 8 we compare the structure factors for DSPC containing 30 mol % PEG-750 and for 100% PEG-350 with those of DSPC incubated in 100 mg/ml ethanol, a condition known to induce the formation of the interdigitated ($L\beta I$) gel phase (Simon and McIntosh, 1984). These comparisons showed that the structure factors of DSPC containing 30 mol % PEG-750 and for 100% PEG-350 were similar to those of DSPC in an interdigitated phase. The differences between the transform of the interdigitated phase of DSPC (Fig. 8, solid

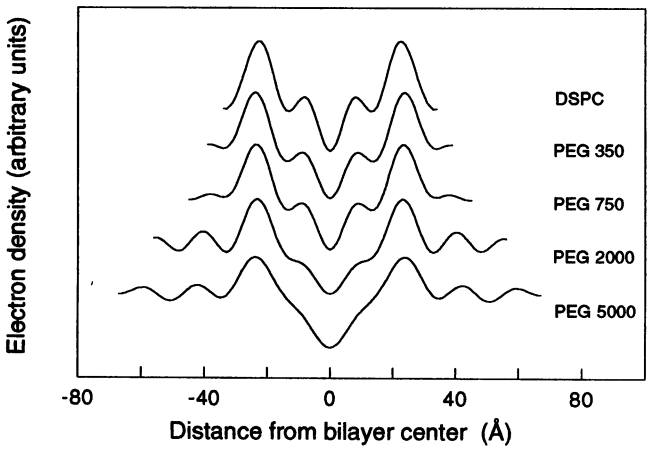

FIGURE 7 Electron density profiles for DSPC bilayers in the absence and presence of 15 mol % PEG-lipid. One unit cell is shown for each profile. PEG-lipid molecular weights are indicated on the figure. All electron density profiles were obtained for applied pressures in the range of 1.1×10^7 to 1.7×10^7 dyn/cm^2.

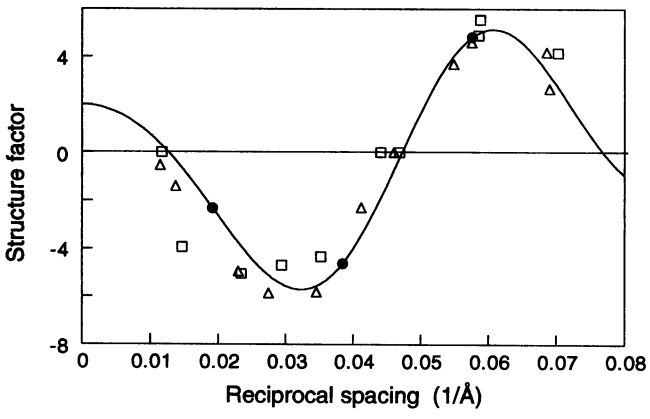

FIGURE 8 Structure factors versus reciprocal space coordinates for: DSPC in 0.1 M ionic strength buffer containing 100 mg/ml ethanol (●), 100 mol % PEG-350 (△), and DSPC containing 20 to 30 mol % PEG-750 (□). The solid line represents the continuous Fourier transform of the interdigitated gel phase calculated using the sampling theorem for the DSPC/ethanol data set.

line) and the structure factors of DSPC:PEG-lipids in the interdigitated phase (particularly between 0.01 and 0.025 $Å^{-1}$) likely arise because PEG increases the density of the fluid space between bilayers, as shown for the Lβ' phase (Fig. 6).

Electron density profiles for DSPC in the absence and presence of 100 mg/ml ethanol, and for DSPC suspensions containing 30 mol % PEG-750 and 100 mol % PEG-350 are shown in Fig. 9. The electron density profiles for DPSC in the presence of ethanol, 30% PEG-750, and 100% PEG-350 differed from the profile of the normal (Lβ') gel phase of DSPC in that the distance between headgroup peaks was only 32.6 ± 0.8 Å (N = 4), or about 15 Å smaller than that observed for Lβ' DSPC bilayers (Fig. 9). Moreover, these profiles (Fig. 9) contained no terminal methyl trough in the center of the bilayer. The shape of these profiles, the distance between head group peaks in the profiles, and the sharp wide-angle reflection at 4.05 Å are all consistent with these bilayers having fully interdigitated hydrocarbon chains (Ranck et al., 1977; McIntosh et al., 1983).

Since the presence of high concentrations of ethylene glycol also causes the formation of the interdigitated phase in gel phase PC bilayers (McIntosh et al., 1983), we tested whether an impurity in the PEG-lipids could be responsible for the formation of the LβI phase in our samples. This possibility was eliminated since interdigitated bilayers were formed when the PEG-lipid was hydrated in a very large excess volume (5 mg/ml) of stressing solution. Thus the formation of the interdigitated phase in DSPC:PEG-lipid suspensions containing high concentrations of PEG-350 or PEG-750 appears to result from properties intrinsic to PEG-350 and PEG-750.

Bilayer phases

The wide-angle and low-angle diffraction data indicate that gel phase bilayers with tilted hydrocarbon chains, similar to the Lβ' phase, were present for DSPC:PEG-lipid suspensions in excess buffer containing 0 to 15 mol % PEG-350, PEG-750, or PEG-2000, or 10 mol % PEG-5000. Both the wide-angle and low-angle diffraction indicated that the interdigitated LβI phase was present for 60–100 mol % PEG-350 or 30–40 mol % PEG-750. For DSPC:PEG-lipid samples containing 20–40 mol % PEG-350 or 15–20 mol % PEG-750, we argue that the presence of both a very sharp 4.05 Å reflection (characteristic of an LβI phase) and a reflection at 4.22 Å (characteristic of an Lβ' phase) (Table 1) indicated that two bilayer phases were present, a normal gel (Lβ') phase and an interdigitated (LβI) phase. The relative intensities of these wide-angle reflections indicated that the Lβ' phase was the dominant phase present at the lower end of these concentration ranges, whereas the LβI phase was more prevalent at the higher end of these concentration ranges. For the 20–40 mol % PEG-350 and 15–20 mol % PEG-750 samples, although the wide-angle patterns indicated that tilted (Lβ') and interdigitated (LβI) gel phases coexisted, a single lamellar repeat period, corresponding to the Lβ' phase, was observed in the low-angle diffraction. Thus, the wide-angle diffraction is a more sensitive indicator of the initial formation of the LβI structure than is the low-angle diffraction. Tristram-Nagle et al. (1994) found a similar result when investigating the formation of the subgel phase.

DSPC:PEG-lipid suspensions containing 20–40 mol % Avanti PEG-2000 or 20–70 mol % Liposome Tech PEG-5000 or 20 to 30 mol % Avanti PEG-5000 gave a single sharp wide-angle reflection at 4.07 Å (Table 1), consistent with the presence of untilted gel phase bilayers. However, these suspensions, as well as suspensions containing 20–50 mol % PEG-2000, did not appear to form an interdigitated phase, since the discrete low-angle reflections had intensity maxima at spacings similar to locations of peaks in the continuous transform of the normal gel phase bilayers (Fig. 5). Thus, for these specimens we argue that the change in the wide-angle pattern with increasing PEG-lipid (Table 1) represents a shift from tilted (Lβ') bilayers to non-interdigitated, untilted (Lβ) bilayers.

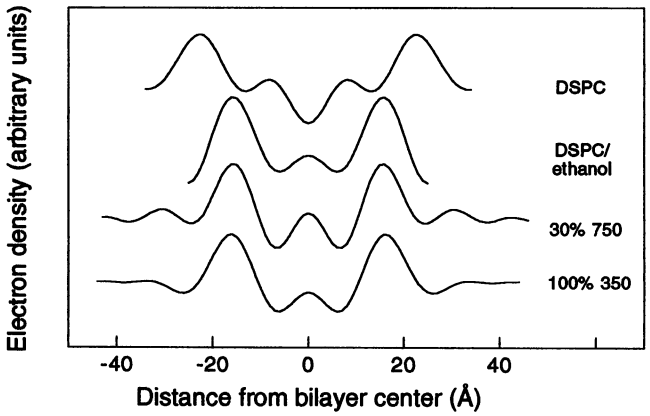

FIGURE 9 Electron density profiles of DSPC (applied pressure = 1.0×10^6 dyn/cm^2), DSPC in the presence of 100 mg/ml ethanol (no applied pressure), DSPC plus 30 mol % PEG-750 (applied pressure = 2.5×10^4 dyn/cm^2), and PEG-350 (applied pressure = 1.0×10^5 dyn/cm^2). One unit cell is shown for each profile.

Interbilayer separations

Since the structure of the bilayer phases in the DSPC:PEG-lipid suspensions was established by these x-ray experiments, we could 1) determine the width of the phospholipid bilayer and 2) estimate the distance between apposing bilayers as a function of both the concentration and molecular weight of the PEG-lipid. The bilayer width was derived from the electron density profiles (Figs. 7 and 9) as follows. Since at this resolution the high density head group peaks in the electron density profile are known to be located between the phosphate moiety and the glycerol backbone of the lipid (Lesslauer et al., 1972; Hitchcock et al., 1974), the profiles in Figs. 7 and 9 can be used to estimate the location of the lipid/water interface. As noted previously (McIntosh and Simon, 1986; McIntosh et al., 1987, 1989a, 1992), the defi-

nition of the lipid/water interface is somewhat arbitrary, because the bilayer surface is not smooth, the lipid head groups are mobile (Hauser, 1981), and water penetrates into the head group region of the bilayer (Worcester and Franks, 1976; Simon et al., 1982; Wiener et al., 1989). We operationally defined the bilayer width as the total thickness of the phosphatidylcholine bilayer assuming that the head group conformation is the same as it is in single crystals of dimyristoylphosphatidylcholine (Pearson and Pascher, 1979). That is, we assumed that the phosphocholine group is, on average, oriented approximately parallel to the bilayer plane, so that the edge of the bilayer lies about 5 Å outward from the center of the high density peaks in the electron density profiles (McIntosh and Simon, 1986; McIntosh et al., 1987). Thus, we estimated the total phospholipid bilayer thickness (d_b) to be the distance between head group peaks in the profiles plus 10 Å.

With these assumptions about bilayer structure, the phospholipid bilayer thickness was estimated to be 57 Å for the tilted (Lβ') gel bilayers (Fig. 7) and 43 Å for the untilted interdigitated bilayers (Fig. 9). We did not obtain diffraction data at sufficient resolution to calculate electron density profiles for DSPC:Avanti PEG-2000, DSPC:PEG-5000, or DSPC:Avanti PEG-5000 suspensions at 20 mol % PEG lipid and higher, for which the wide-angle data (Table 1) indicated that untilted Lβ gel phase bilayers with reduced hydrocarbon chain tilt were present. For these specimens, we assumed a bilayer thickness of 63 Å, since an increase in bilayer thickness of about 6 Å should be associated with a reduction of hydrocarbon chain tilt from 30 to 0 degrees. The thickness of the fluid layer between adjacent bilayers (d_f) was obtained by subtracting the appropriate values of d_b defined above from the lamellar repeat periods (Fig. 4).

A plot of d_f versus concentration of PEG-lipid as a function of PEG molecular weight is shown in Fig. 10 for a constant applied osmotic pressure of 1×10^5 dyn/cm^2. For all four PEG-lipids, the width of the fluid space increased with increasing mol fraction PEG-lipid until a maximum was attained at about 10–15 mol % PEG-lipid. At this applied pressure, the limiting fluid separation between bilayers was a strong function of PEG-lipid, being about 40 Å for PEG-350, 55 Å for PEG-750, 120 Å for PEG-2000, and 200 Å for PEG-5000.

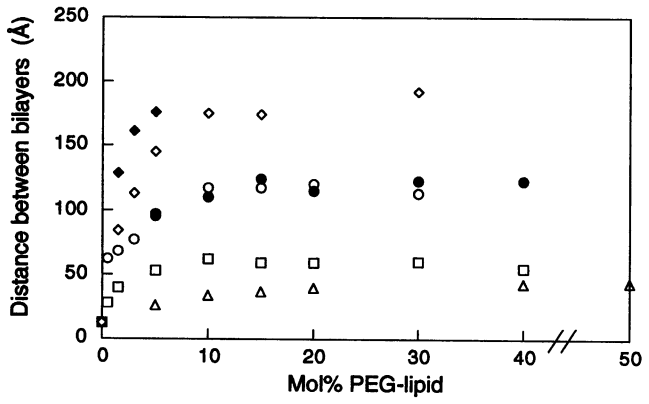

FIGURE 10 Distance between apposed DSPC:PEG-lipid bilayers as a function of mol % PEG-lipid at an applied pressure of 1.0×10^5 dyn/cm^2 for PEG-350 (△), PEG-750 (□), PEG-2000 (●), and PEG-5000 (◇), Avanti PEG-2000 (●), and Avanti PEG-5000 (◆).

The 15 Å decrease in repeat period observed for PEG-750 between 15 and 20 mol % PEG-750 (Fig. 4) and for PEG-350 between 40 and 100 mol % PEG-350 was not present in the plot of fluid thickness versus mol % PEG-lipid (Fig. 10) because that decrease was due to the difference in bilayer thickness of the Lβ' phase and the interdigitated LβI phase. After correcting for differences in bilayer thickness with the change in phase from tilted to interdigitated bilayers for PEG-350 and PEG-750, the fluid space remained approximately constant with increasing PEG-350 or PEG-750 concentration above 15 mol %.

NMR

^{1}H NMR was used to assess the phase of hydrated DSPC:PEG-lipid suspensions at temperatures above (70°C) and below (28°C) the main endothermic phase transition temperatures (from Fig. 2). We initially consider the spectra of aqueous dispersions of DSPC and PEG-lipids and then DSPC:PEG-lipid mixtures.

Fig. 11 shows ^{1}H spectra at 28 and 70°C for DSPC and PEG-2000 in 20 mM HEPES, 100 mM NaCl, pD 7, prepared in D_2O. All the spectra contained peaks from the HEPES buffer (2.9, 3.2, and 3.9 ppm) and water proton resonances (4.7 ppm at 28°C or 4.3 ppm at 70°C). Assignments for the major phospholipid hydrocarbon and PEG resonances are shown. For DSPC suspensions at 28°C (Fig. 11 *A*) only resonances associated with HEPES and water were observed. For DSPC at 70°C (Fig. 11 *B*) the proton spectra contained two additional broad peaks (at 0.85 and 1.35 ppm) that are characteristic of the terminal methyl and hydrocarbon chains, respectively, of liquid crystalline bilayers (Finer et al., 1972). Thus the ^{1}H-NMR spectra of hydrated DSPC were characteristic of gel phase bilayers at 28°C and liquid crystalline bilayers at 70°C. The ^{1}H NMR spectra for suspensions of PEG-2000 (Fig. 11, *C* and *D*) and for PEG-750 and PEG-5000 (data not shown) were considerably different from those of DSPC in either the gel or liquid crystalline phases. First, for suspensions of PEG-2000 at both 28°C (Fig. 11 *C*) and 70°C (Fig. 11 *D*) strong resonance was observed at 3.73 ppm, a position characteristic of the (O—CH_2—CH_2)$_n$ protons in PEG (Ribeiro and Dennis, 1987). We confirmed this assignment by obtaining a spectrum of a 5 mM solution of polyethylene glycol with a molecular weight of 3336 Da (data not shown). Second, at both 28 and 70°C, several relatively sharp proton resonances associated with the hydrocarbon region of the lipid were apparent, including peaks at 1.65 ppm (CH_2—C—COO of hydrocarbon), 1.3 ppm (hydrocarbon methylenes), 0.9 ppm (terminal methyls), and 2.35 ppm (C—CH_2—COO of hydrocarbon), as well as peaks at 4.2 and 4.4 ppm, which are associated with protons in the glycerol backbone region of the lipid (Finer et al., 1972). The presence of such narrow hydrocarbon resonances is characteristic of solubilized phospholipid (Sparling et al., 1989) or

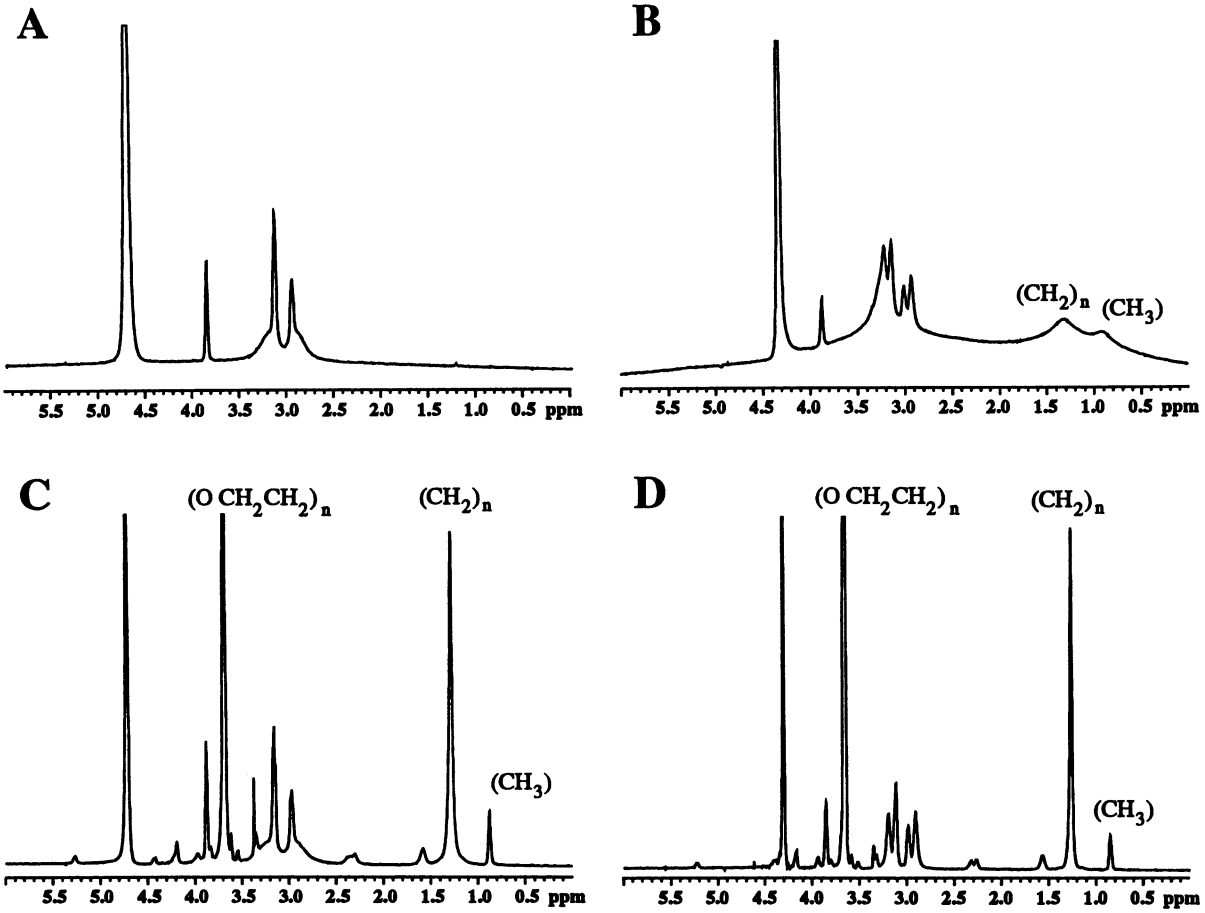

FIGURE 11 ^{1}H NMR spectra for suspensions containing (*A*) 50 mM DSPC at 28°C; (*B*) 50 mM DSPC at 70°C; (*C*) 5 mM PEG-2000 at 28°C; and (*D*) 5 mM PEG-2000 at 70°C. The major lipid resonances are labeled.

lipids organized either as micelles (Ribeiro and Dennis, 1975) or SUVs (Finer et al., 1972). Since the hydrocarbon resonances for the PEG-2000 dispersion were essentially identical at 28 and 70°C, we argue that these isotropic PEG-2000 hydrocarbon ^{1}H resonances are here associated with micelles rather than SUVs. This interpretation is consistent with the absence of a bilayer melting transition in the calorimetry measurements (Fig. 3).

Representative ^{1}H spectra for several DSPC:PEG-2000 dispersions are shown in Fig. 12. The spectra for 10 mol % PEG-2000 (Fig. 12, *A* and *B*) were similar to those of pure DSPC bilayers (Fig. 11, *A* and *B*) in that at 28°C no resonances were observed below 2 ppm, whereas at 70°C two broad resonances appeared in this region. These results indicated that at 10 mol % PEG-2000, the sample contained a pure bilayer phase. In contrast, at 30 mol % PEG-2000, broad resonances were observed at 0.9 and 1.3 ppm at 28°C (Fig. 12 *C*), and sharp resonances were observed at 0.9, 1.3 and 1.65 ppm at 70°C (Fig. 12 *D*). These resonances at 70°C were similar to those obtained in the PEG-2000 sample at 70°C (Fig. 11 *D*). In addition, a sharp peak was present at 3.25 ppm (Fig. 12), which was not present in the DSPC suspensions or pure PEG-2000 micelles at this temperature (Fig. 11). This resonance occurred at a position characteristic for choline (Finer et al., 1972; Ribeiro and Dennis, 1975; Sparling et al., 1989), although it was difficult to unambiguously assign because it fell close to a HEPES resonance. Based on these observations, we argue that at 30 mol % PEG-2000, a portion of the sample existed as an isotropic phase containing both PEG-lipid and DSPC.

The presence of a strong, narrow PEG resonance at 3.73 ppm is associated with both bilayer and micelle phases (Figs. 11 and 12). Thus it appears that, even when attached to a bilayer surface, at least a portion of the PEG molecule demonstrates motion comparable to that of the molecule in solution.

Phase diagrams

In Fig. 13, *A–D* we present phase diagrams for DSPC:PEG-lipid suspensions containing PEG-350, PEG-750, PEG-2000, and PEG-5000, respectively. (Phase diagrams for DSPC with Avanti PEG-2000 and Avanti PEG-5000 were similar to those shown in Fig. 13 *D*, although less extensive data were collected with the Avanti lipids.) The lipid structures indicated in these phase diagrams are shown schematically in Fig. 14. The phase transition temperatures were determined from differential scanning calorimetry, and are

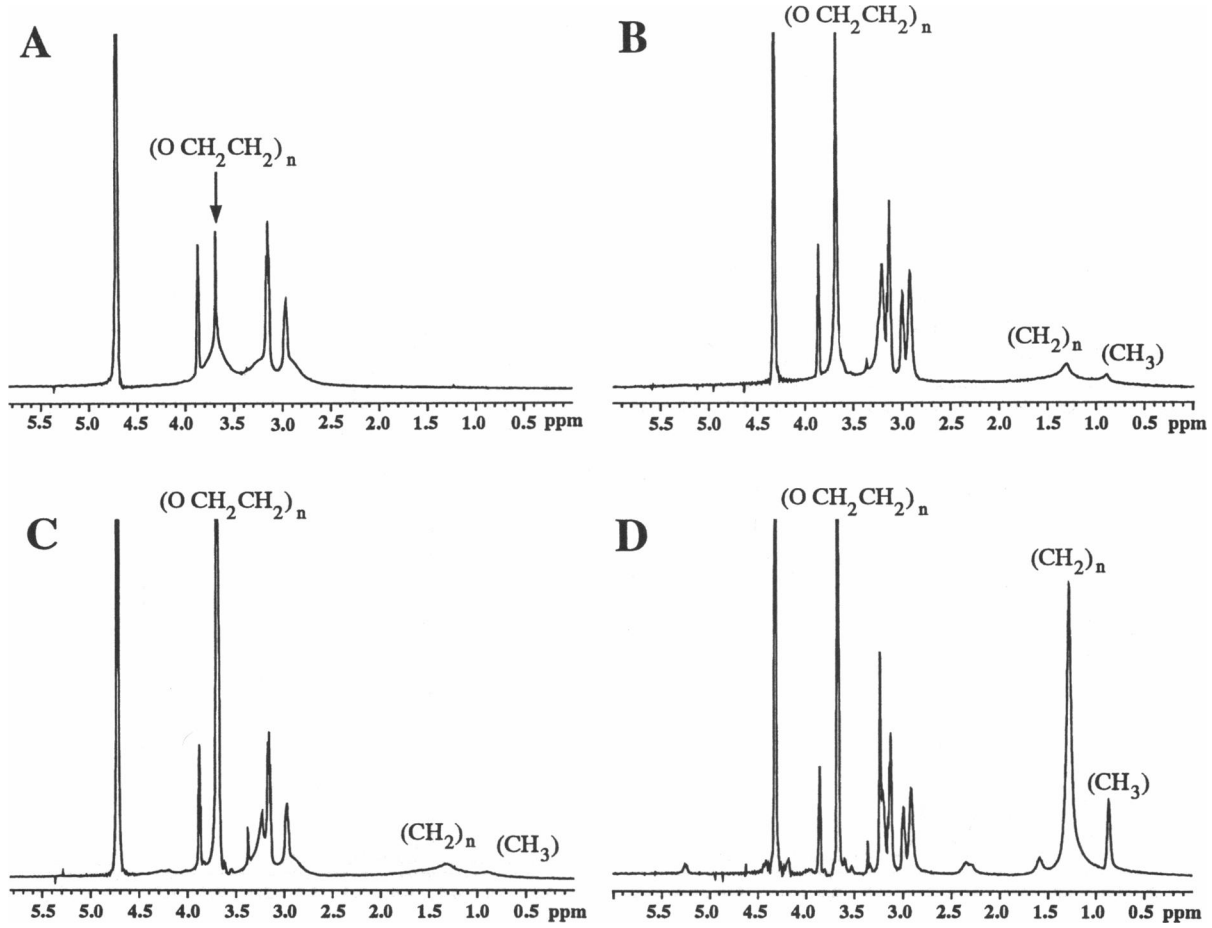

FIGURE 12 ^{1}H NMR spectra for DSPC:PEG-2000 dispersions containing (*A*) 10 mol % PEG-2000 (13.6 mM total lipid) at 28°C, (*B*) 10 mol % PEG-2000 (13.6 mM total lipid) at 70°C, (*C*) 30 mol % PEG-2000 (9.9 mM total lipid) at 28°C, and (*D*) 30 mol % PEG-2000 (9.9 mM total lipid) at 70°C. The major lipid resonances are labeled.

shown as solid lines through the data points. The structures above the main transition temperature were determined by light microscopy and NMR data, and the structures below the main transition temperature were determined by the light microscopy, absorbance measurements, x-ray diffraction, and NMR data described above. These various techniques provide complementary information. For example, the wide-angle and low-angle x-ray diffraction data are sensitive to the presence of bilayer phases, whereas the NMR spectra contain specific resonances characteristic of micelles. However, the positions of the vertical boundaries, in particular the boundaries of the two phase bilayer plus micelle regions, have not been precisely determined because: 1) we performed the x-ray experiments at only one temperature and the NMR experiments at only two temperatures, and 2) because we ignored the relatively small amount of water in the PEG-lipids in gravimetric preparations of the lipid mixtures. Therefore, the broad two phase regions are shown as hatched areas with indistinct boundaries.

In all methods except for some of the x-ray diffraction experiments, the phase diagrams were obtained at full hydration. For the x-ray experiments designed to determine the bilayer structure ($L\beta'$ or $L\beta I$), osmotic pressures (up to 1.5 $\times$ 10^7 dyn/cm^2) were applied to squeeze adjacent bilayers together to improve the orderliness of the lamellar arrays. Previously it has been shown in the case of phosphatidylcholine bilayers that such applied pressures remove some interbilayer water, but have little effect on bilayer structure (McIntosh and Simon, 1986). However, more extensive removal of water substantially modifies the phase diagrams. For example, at low water contents (<50% water), pure PEG-750 forms bilayers rather than micelles (data not shown). In addition, as shown in the accompanying paper (Kenworthy et al., 1995), the value of lamellar repeat period and the length of extension of the polymer from the bilayer surface in DSPC:PEG-lipid bilayers depend importantly on water content (applied pressure).

The phase diagrams presented in Fig. 13 have several features in common. For all DSPC:PEG-lipid systems at low PEG-lipid concentrations, $P\beta'$ and $L\beta'$ gel phase bilayers were present below the main phase transition temperature and liquid crystalline ($L\alpha$) phase bilayers were present at temperatures above the main melting transition. However, there are three important differences in the phase diagrams at higher PEG-lipid concentrations. First, the bilayer structure depended strongly on the PEG-lipid's molecular weight

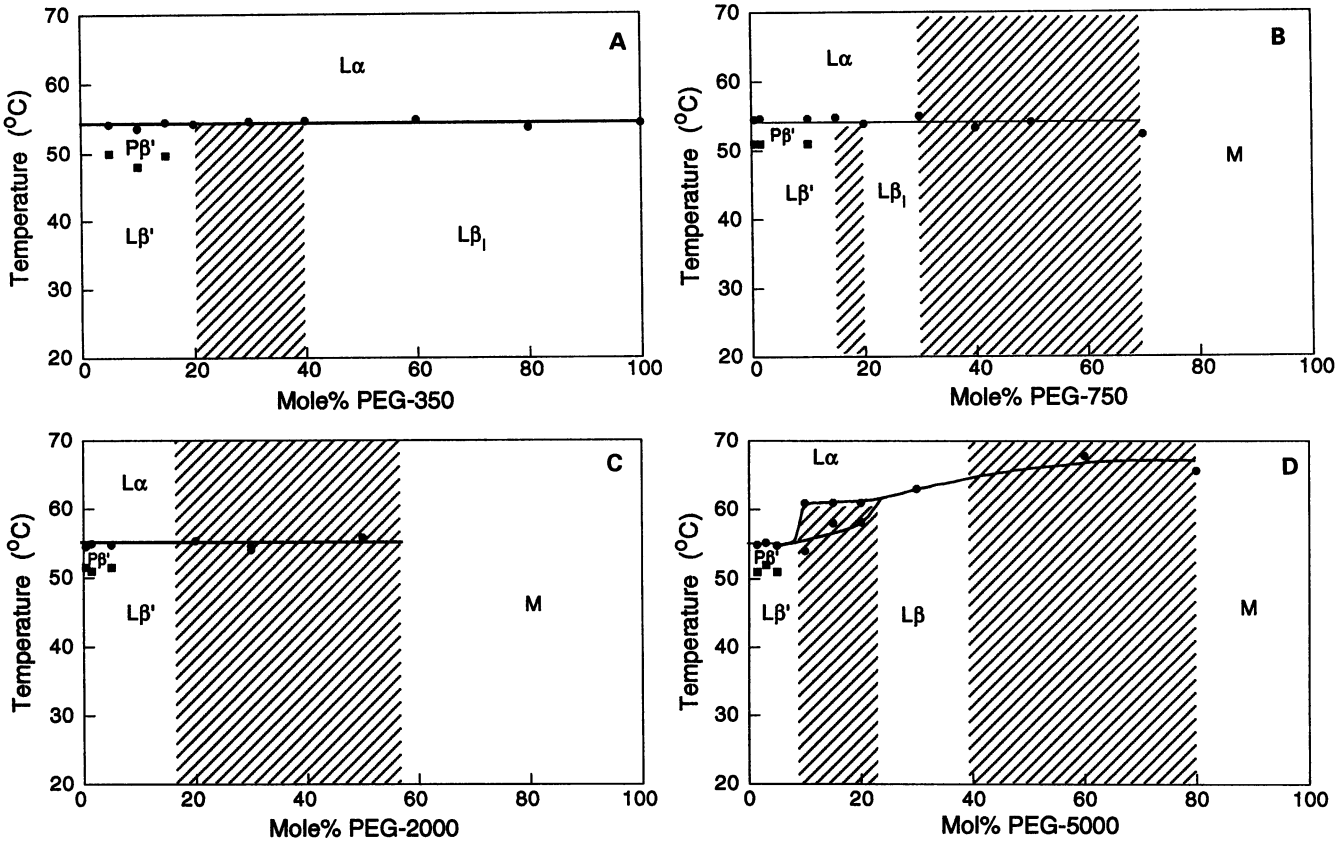

FIGURE 13 Phase diagrams for DSPC:PEG-lipid dispersions for (*A*) DSPC:PEG-350, (*B*) DSPC:PEG-750, (*C*) DSPC:PEG-2000, and (*D*) DSPC:PEG-5000. The solid lines are drawn to guide the eye through the T_m values (●) obtained by DSC. The hatched regions indicate two phase regions whose phase boundaries are approximate.

for PEG-lipid concentrations greater than 20 mol %. Specifically, for DSPC suspensions containing PEG-350 and PEG-750 the bilayer structure changed from a tilted gel phase (Lβ′) to an interdigitated gel phase (LβI) at concentrations greater than about 40 mol % PEG-350 and 20 mol % PEG-750 (Figs. 13, *A* and *B*, 14), whereas an untilted, uninterdigitated (Lβ) bilayer was formed above about 20 mol % PEG-5000 (Figs. 13 *D*, 14). Second, whereas the main phase

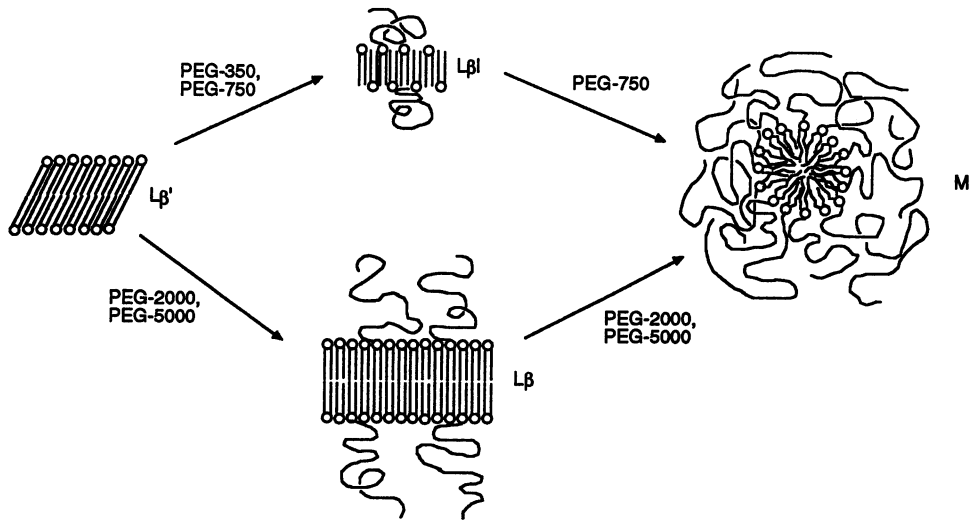

FIGURE 14 Schematic diagram of the lipid phases (as indicated in Fig. 13) assumed by DSPC:PEG-lipid dispersions at 20°C. Structures are not drawn to scale. Note that the Lβ phase was observed for DSPC suspensions containing Avanti PEG-2000 but not for suspensions containing Liposome Technology PEG-2000.

transition temperature remained constant for DSPC:PEG-lipid dispersions containing 0 to 100 mol % PEG-350 and from 0 to 60 mol % PEG-750 and PEG-2000, it increased for the DSPC:PEG-5000 dispersions. Moreover, for DSPC:PEG-5000 dispersions containing between 10 and 20 mol % PEG-lipid there were two thermal transitions. This provided good evidence for a two phase region between the gel and liquid crystalline phases in this region of the phase diagram (Fig. 13 *D*). For DSPC:PEG-5000 dispersions containing greater than 20 mol % PEG-lipid only a single endothermic transition was present. The presence of this high temperature transition was directly correlated with the shift from a normal $L\beta'$ wide angle pattern to a single 4.05 or 4.07 Å wide-angle reflection (Table 1), which we argue arises from an $L\beta$ bilayer phase. Third, although DSPC:PEG-350 (Fig. 13 *A*) formed bilayers across the entire concentration range, the other DSPC:PEG-lipids dispersion formed micelles at high PEG-lipid concentrations (Figs. 13, *B–D* 14). The presence of micelles (shown as "M" in Figs. 13 and 14) at large concentrations of PEG-750, PEG-2000, and PEG-5000 was indicated by the following observations. The light microscopy, absorbance, and NMR measurements indicated that large concentrations of these PEG-lipids converted MLVs into small, non-birefringent structures, such as micelles or perhaps SUVs. However, for these PEG-lipid concentrations at 20°C, the absence of sharp wide-angle reflections indicates the absence of gel phase SUVs (Table 1) as does the presence of the sharp NMR resonances at 0.9 and 1.3 ppm. Finally, since SUVs have similar transition temperatures to MLVs whereas micelles do not have endothermic transitions, the loss in the enthalpy and eventual absence of thermal transitions at high concentrations of PEG-750, PEG-2000, and PEG-5000 provide strong evidence that micelles were present under these conditions. However, we cannot rule out the possibility that a small contribution to the reduction in enthalpy, especially at the higher PEG-lipid concentrations, could arise from an exothermic reaction resulting from increased hydration of the PEG upon melting of the acyl chains.

DISCUSSION

In this paper several biophysical techniques have been used to determine the structure and phase behavior of DSPC:PEG-lipid suspensions. Here we consider the manner in which PEG-lipids modify the structure and properties of DSPC liposomes, and discuss how these results help to explain the mechanisms whereby PEG-lipids increase the blood circulation time of the PEG-liposomes.

Structure and thermal properties of DSPC:PEG-lipid suspensions

The phase diagrams for the DSPC:PEG-lipids (Fig. 13) are all similar for PEG-lipid concentrations up to about 10 mol %. However, for PEG-lipid concentrations above 10 mol % the phase diagrams for the specific PEG-lipids differ in the structure and thermal properties of the lipid phase. Below we consider the factors contributing to the differences in lipid phase, discuss the differences in the thermal properties of the bilayer phases, and finally compare our PEG-lipid phase diagrams to those reported previously.

In terms of the first point, interdigitated bilayers are formed in the presence of high concentrations of PEG-350 and intermediate concentrations of PEG-750, whereas micelles are formed with high concentrations of PEG-750, PEG-2000, and PEG-5000 (Fig. 13). Since all of the PEG-lipids are negatively charged at pH 7 and have the same acyl chain composition, neither lipid charge nor hydrocarbon chain differences can account for whether an interdigitated bilayer or micelle is formed by the addition of a PEG-lipid. The obvious difference among the various PEG-lipids is the relative size, or bulkiness, of the covalently attached PEG. We thus consider the shape and size of polar molecules that, when added to PC bilayers, induce the formation of either interdigitated phase bilayers or micelles. For gel ($L\beta'$) phase PCs, the formation of the interdigitated phase can be induced by the addition of surface-active molecules (McDaniel et al., 1983) such as short-chain alcohols (Simon and McIntosh, 1984; Rowe, 1987), which partition into the headgroup/solvent interfacial region without penetrating deeply into the hydrocarbon region. The mechanism by which these molecules are thought to induce the formation of the interdigitated phase involves wedging apart the headgroups in the plane of the bilayer, thereby increasing the excluded area of the headgroup relative to the excluded area of the hydrocarbon chains (McDaniel et al., 1983; Simon and McIntosh, 1984). The lipid hydrocarbon chains from apposing monolayers of the bilayer interpenetrate to maximize van der Waals interactions. For the interdigitated ($L\beta I$) phase compared with the ($L\beta'$) phase, the gain in energy due to increased van der Waals interactions between the acyl chains is sufficient to compensate for the energy required to expose terminal methyl groups to water (Simon and McIntosh, 1984; Simon et al., 1986). Moreover, for charged surface-active molecules, such as the PEG-lipids, the interdigitated phase is energetically favored over the $L\beta$ or $L\beta'$ phases in terms of the electrostatic interactions, since it has about half the surface charge density. The conversion of PC bilayers to micelles is caused by the addition of "cone-shaped" or "wedged-shaped" molecules (Israelachvili et al., 1977, 1980), such as detergents or lysolipids. In these wedge-shaped molecules the excluded area of the head group is larger than the excluded area of the hydrocarbon region of the molecule. In general, such wedge-shaped molecules tend to form micelles by themselves when fully hydrated.

We argue, therefore, that the relative "shape" of the various PEG-lipids must be a key factor in the differences in observed phase behavior of the DSPC:PEG-lipid suspensions at high PEG-lipid concentrations. The larger the size

of the attached PEG, the more wedge-shaped is the PEG-lipid. For comparison, the molecular weight of the DSPC head group is <300 Da. Therefore, the size of the PEG in PEG-350 is somewhat larger, and the size of the PEG in PEG-5000 is much larger, than the head group of DSPC. Thus, the wedge-shaped PEG-2000 and PEG-5000 molecules form micelles in solution and act like detergents in that they convert DSPC to micelles at high PEG-lipid concentrations (Fig. 13, *C* and *D*). In contrast, PEG-350, which forms bilayers in solution and is more cylindrical and less wedge-shaped, is able to separate the PC head groups enough to cause interdigitation at high PEG-350 concentrations, but not enough to cause micelle formation even in dispersions containing pure PEG-350 (Fig. 13 *A*). PEG-750 has an intermediate shape, so that when added to DSPC it induces interdigitated bilayers at moderate concentrations and mixed micelles at higher concentrations (Fig. 13 *B*).

A problem with this "shape" model analysis is that it does not explain why intermediate concentrations of PEG-2000 and PEG-5000 form Lβ bilayers, rather than LβI bilayers. Although we do not know the reasons for this observation, a complicating factor in this type of "shape" analysis is that the conformation of the PEG-lipid head group depends on the size of the PEG head group and the concentration of PEG-lipid in the bilayer (Kenworthy et al., 1995). For the case of intermediate concentrations of either PEG-2000 or PEG-5000 in the bilayer, the neighboring PEG chains come into contact and change their conformation from a rounded "mushroom" to an extended or cylindrical "brush" (Kenworthy et al., 1995). Therefore, another factor that may be involved in the conversion of Lβ' phase bilayers to either Lβ bilayers, LβI bilayers, or micelles is the conformation of the initial segments of the polymer chains (near the bilayer interface), that might be different for PEG-350 or PEG-750 in comparison to PEG-2000 or PEG-5000.

In a theoretical approach to understanding PEG-lipid phase behavior, Hristova and Needham (1995) formulated a model for the phase behavior of PEG-lipid/phospholipid systems based on the free energy of bilayers containing laterally interacting polymers. This analysis also calculated the limiting concentration of PEG-lipid that can be incorporated in a bilayer phase in terms of lateral interactions between the grafted polymers as balanced by either 1) the material properties of the bilayer or 2) the energetics of the polymorphic behavior of the lipid matrix. Experimental tests of these theoretical models for PEG-lipid saturation limit in the bilayer will be presented in a separate paper (K. Hristova, A. K. Kenworthy and T. J. McIntosh, manuscript in preparation).

The calorimetry data can be understood primarily in terms of the structures of the various phases shown in the phase diagram (Fig. 13). First, as noted above, the loss of enthalpy with increasing PEG-750, PEG-2000, and PEG-5000 concentration can be explained in terms of conversion of the Lβ' bilayer phase to a mixed micellar phase. Second, the increase in the main transition temperature with increasing Avanti PEG-2000 (but not Liposome Technology PEG-2000), Avanti PEG-5000, PEG-5000, and the constant T_m with increasing concentrations of PEG-350 and PEG-750, can be rationalized at least qualitatively, by the structure of the gel phase bilayers. The shift from Lβ' to either Lβ or LβI produces closer hydrocarbon chain packing, as indicated directly by the smaller wide-angle spacings (Table 1). This shift stabilizes the gel phase by increasing van der Waals interactions, and therefore would be expected to increase T_m compared with the Lβ' phase. This is, in fact, the effect seen for PEG-5000 Lβ bilayers (Fig. 13 *D*). However, the exposure of hydrocarbon to water in the LβI phase would be expected to destabilize the gel phase, and thus LβI bilayers would be expected to melt at a lower temperature than untilted gel phase bilayers (Lβ), as observed (Fig. 13, *A* and *B*). It should be noted that PEG-350 bilayers melt at a temperature about 20°C below the main endothermic transition temperature of bilayers of DSPE, the molecule to which the PEG chain is attached in PEG-lipids. Three factors are likely involved in this reduction in phase transition temperature: 1) the formation of the LβI phase, as described above, 2) the charge on the PEG-lipid, and 3) the bulkiness of the PEG-lipid head group. In terms of the latter two points, previous experiments have shown that either increasing the surface charge on PE bilayers by changing the pH or increasing the size of the PE head group by methylation decreases the phase transition temperature (Cevc, 1987). Moreover, biotinylated DSPE, which like PEG-lipids has a single negative charge and a more bulky head group, has a phase transition 20–30°C lower than that of DSPE, depending on the NaCl concentration in the buffer (Swamy et al., 1994).

Two previous studies have examined the phase behavior of mixtures of phospholipid and PEG-lipid. Lasic et al. (1991b) used light microscopy and light scattering to look at the phase behavior of liquid-crystalline phase egg lecithin: PEG-2000 mixtures at room temperature. They argued that egg lecithin:PEG-2000 forms bilayers for PEG-2000 contents <60 mol % and micelles for PEG-2000 contents >60 mol %. We also observe the formation of micelles at high PEG-2000 concentrations. A phase diagram constructed from differential scanning calorimetry and polarization measurements has also been reported for DSPC:PEG-5000 (Blume and Cevc, 1993). Our results for PEG-5000 are similar to those of Blume and Cevc (1993), in that they reported an increase in the main transition temperature from 55 to 68°C, accompanied by a significant drop in enthalpy, as PEG-5000 concentration was increased from 0 to 50 mol %. Our results differ, however, in that while Blume and Cevc (1993) reported a "melting" of pure PEG-5000 at 65°C, consistent with the presence of a bilayer phase, our absorbance, light microscopy, calorimetry, x-ray diffraction, and NMR results (Figs. 1–3, Table 1) all point to the formation of a micellar phase in fully hydrated PEG-5000. A possible reason for this difference in results may be that Blume and Cevc (1993) were examining a partially hydrated system. Furthermore, they did not mention the possibility that a mixed-phase region is present above 15 mol % PEG-5000, although both their data and our data indicate the presence of a broad two phase region.

Implications for drug delivery and grafted polymer theory

The results of this study provide additional information for understanding the physical basis of the effect of the incorporation of PEG-lipid on blood circulation times and the therapeutic efficiency of liposomal drug delivery systems. The blood circulation time of PEG-liposomes has been shown to depend strongly on both the molecular weight of the PEG and the concentration of PEG-lipid (Mori et al., 1991; Woodle et al., 1992) and it has been shown that the large increase in fluid space observed in the presence of the PEG-lipid must arise from a steric interaction between apposed PEG headgroups (Needham et al., 1992; Kenworthy et al., 1995).

Our results, summarized in Figs. 10, 13, and 14, help to explain two specific observations of the effects of PEG-lipids on drug circulation time. First, it has been observed that PEG-liposome blood circulation times increase as PEG molecular weight is increased from 750 to 2000 or 5000 (Mori et al., 1991; Woodle et al., 1992). These results can be rationalized in terms of steric barrier model, since we observe that the range of the steric barrier increases with increasing PEG size. Moreover, our experiments (Fig. 10) provide an estimate for the minimum range of the steric barrier necessary to substantially increase liposome circulation times. Second, the effect of PEG-lipid on blood circulation appears to depend on the concentration of PEG-lipid in the liposome, reaching a maximum effect near 10 mol % PEG-lipid (Woodle and Lasic, 1992). We find that the range of the steric barrier provided by the incorporation of PEG-lipid also reaches a maximum near 10 mol % (Fig. 10). The addition of higher concentrations of PEG-lipid does not further increase the range of the steric barrier (Fig. 10), and, in the cases of PEG-2000 and PEG-5000, larger concentrations of the PEG-lipid would be detrimental to drug delivery, since they break up the liposomes to form micelles (Fig. 13).

Our results also establish the applicability of the osmotic stress/multilamellar PEG liposome system for extending theories of the behavior of surface-grafted polymer to the relatively small polymers used in these studies. Such theories (Alexander, 1977; deGennes, 1988; Milner, 1991) predict that polymer "grafting density" and size both contribute importantly to the conformation and interactive properties of surface-grafted polymers. The results reported in this paper show that the extended length of the PEG from the bilayer surface depends strongly on both PEG size and PEG-lipid concentration in the bilayer for PEG-lipid concentrations up to about 10 mol % (Fig. 10). Based on these results, we argue that this system represents a powerful experimental tool for further testing these theories, and in the accompanying paper (Kenworthy et al., 1995) we present a full characterization of the range and magnitude of the steric polymer-polymer interactions in this system.

We thank Dr. David Needham for acquainting us with PEG-lipids and for many helpful suggestions during the course of this work. We also thank Dr. Kalina Hristova for helpful discussions, Dr. Anthony Ribeiro for assistance with the NMR experiments, Dr. Klaus Gawrisch for helpful suggestions concerning the NMR results, and Dr. D. Lasic of Liposome Technology, Inc., for supplying us with the PEG-lipids.

This work was supported by grant GM-27278 from the National Institutes of Health.

REFERENCES

Ahmad, I., M. Longenecker, J. Samuel, and T. M. Allen. 1993. Antibody-targeted delivery of doxorubicin entrapped in sterically stabilized liposomes can eradicate lung cancer in mice. *Cancer Res.* 53:1484–1488.

Alexander, S. 1977. Adsorption of chain molecules with a polar head. A scaling description. *J. Phys. (Paris).* 38:983.

Allen, T. M., A. K. Agrawal, I. Ahmad, C. B. Hansen, and S. Zalipsky. 1994. Antibody-mediated targeting of long-circulating (stealth) liposomes. *J. Liposome Res.* 4:1–26.

Allen, T. M., C. Hansen, F. Martin, C. Redemann, and A. Yau-Young. 1991. Liposomes containing synthetic lipid derivatives of poly(ethyleneglycol) show prolonged circulation half-lives in vivo. *Biochim. Biophys. Acta.* 1066:29–36.

Almog, S., B. J. Litman, W. Wimley, J. Cohen, E. J. Wachtel, Y. Barenholz, A. Ben-Shaul, and D. Lichtenberg. 1990. States of aggregation and phase transformations in mixtures of phosphatidylcholine and octyl glucoside. *Biochemistry.* 29:4582–4592.

Blaurock, A. E., and C. R. Worthington. 1966. Treatment of low angle x-ray data from planar and concentric multilayered structures. *Biophys. J.* 6:305–312.

Blume, G., and G. Cevc. 1990. Liposomes for the sustained drug release in vivo. *Biochim. Biophys. Acta.* 1029:91–97.

Blume, G., and G. Cevc. 1993. Molecular mechanism of the lipid vesicle longevity in vivo. *Biochim. Biophys. Acta.* 1146:157–168.

Blume, G., G. Cevc, M. D. J. A. Crommelin, I. A. J. M. Bakker-Woudenberg, C. Kluft, and G. Storm. 1993. Specific targeting with poly-(ethylene glycol)-modified liposomes: coupling of homing devices to the ends of the polymeric chains combines effective target binding with long circulation times. *Biochim. Biophys. Acta.* 1149:180–184.

Bourges, M., D. M. Small, and D. G. Dervichian. 1967. Biophysics of lipidic associations II. The ternary systems cholesterol-lecithin-water. *Biochim. Biophys. Acta.* 137:157–167.

Bridgett, M. J., M. C. Davies, and S. P. Denver. 1992. Control of staphylococcal adhesion to polystyrene surfaces by polymer surface modification with surfactants. *Biomaterials.* 13:411–416.

Carmona-Riberio, A. M., and H. Chaimovich. 1986. Salt-induced aggregation and fusion of dioctadecyldimethylammonium chloride and sodium dihexadecylphosphate vesicles. *Biophys. J.* 50:621–628.

Cevc, G. 1987. How membrane chain melting properties are regulated by the polar surface of the lipid bilayer. *Biochemistry.* 26:6305–6310.

Claesson, P. M., and C.-G. Gölander. 1987. Direct measurements of steric interactions between mica surfaces covered with electrostatically bound low-molecular weight polyethylene oxide. *J. Colloid Interface Sci.* 117: 366–374.

Costello, B. A. deL., P. F. Luckham, and T. F. Tadros. 1993. Forces between adsorbed low molecular weight graft copolymers. *J. Colloid Interface Sci.* 156:72–77.

deGennes, P. G. 1988. Model Polymers at interfaces. *In* Physical Basis of Cell-Cell Adhesion. P. Bongrand, editor. CRC Press, Boca Raton, Florida.

Desai, N. P., S. F. A. Hossainy, and J. A. Hubbell. 1992. Surface-immobilized polyethylene oxide for bacterial repellence. *Biomaterials.* 13:417–420.

Dolan, A. K., and S. F. Edwards. 1974. Theory of the stabilization of colloids by adsorbed polymer. *Proc. Royal Soc. Lond. A.* 337:509–516.

Finer, E. G., A. G. Flook, and H. Hauser. 1972. Mechanism of sonication of aqueous egg yolk lecithin dispersions and nature of the resultant particles. *Biochim. Biophys. Acta.* 260:49–58.

Hauser, H. 1981. The polar group conformation of 1,2-dialkyl phosphatidylcholines. An NMR study. *Biochim. Biophys. Acta.* 646:203–210.

Herbette, L., J. Marquardt, A. Scarpa, and J. K. Blasie. 1977. A direct analysis of lamellar x-ray diffraction from hydrated oriented multilayers of fully functional sarcoplasmic reticulum. *Biophysical J.* 20:245–272.

Hinz, H.-J., and J. M. Sturtevant. 1972. Calorimetric studies of dilute aqueous suspensions of bilayers formed from synthetic L-α-lecithin. *J. Biol. Chem.* 247:6071.

Hitchcock, P. B., R. Mason, K. M. Thomas, and G. G. Shipley. 1974. Structural chemistry of 1,2 dilauroyl-DL-phosphatidylethanolamine:molecular conformation and intermolecular packing of phospholipids. *Proc. Nat. Acad. Sci. USA.* 71:3036–3040.

Hristova, K., and D. Needham. 1994. The influence of polymer-grafted lipids on the physical properties of lipid bilayers: a theoretical study. *J. Colloid Interface Sci.* 168:302–314.

Hristova, K., and D. Needham. 1995. Phase behavior of a lipid/polymer-lipid mixture in aqueous medium. *Macromolecules.* 28:991–1002.

Israelachvili, J. N., and G. E. Adams. 1976. Direct measurement of long range forces between two mica surfaces in aqueous KNO3 solutions. *Nature.* 262:774–776.

Israelachvili, J. N., S. Marcelja, and R. G. Horn. 1980. Physical principles of membrane organization. *Q. Rev. Biophys.* 13:121–200.

Israelachvili, J. N., J. Mitchell, and B. W. Ninham. 1977. Theory of self-assembly of lipid bilayers and vesicles. *Biochim. Biophys. Acta.* 470: 185–201.

Israelachvili, J. N., R. K. Tandon, and L. R. White. 1979. Measurement of forces between two surfaces in aqueous poly(ethylene oxide) solutions. *Nature.* 277:120–121.

Janiak, M. J., D. M. Small, and G. G. Shipley. 1979. Temperature and compositional dependence of the structure of dimyristoyl lecithin. *J. Biol. Chem.* 254:6068–6078.

Jeon, S. I., J. H. Lee, J. D. Andrade, and P. G. DeGennes. 1991. Protein-surface interactions in the presence of polyethylene oxide. I. Simplified theory. *J. Colloid Interface Sci.* 142:149–158.

Kenworthy, A. K., K. Hristova, D. Needham, and T. J. McIntosh. 1995. Range and magnitude of the steric pressure between bilayers containing phospholipids with covalently attached poly(ethyleneglycol). *Biophys. J.* This issue.

Klein, J., and P. Luckham. 1982. Forces between two adsorbed polyethylene oxide layers immersed in a good aqueous solvent. *Nature.* 300:429–430.

Klein, J., and P. F. Luckham. 1984. Forces between two adsorbed poly-(ethylene oxide) layers in a good aqueous solvent in the range 0–150 nm. *Macromolecules.* 17:1041–1048.

Klein, J., and P. Pincus. 1982. Interaction between surfaces with adsorbed polymers: poor solvents. *Macromolecules.* 15:1129–1135.

Klibanov, A. L., and L. Huang. 1992. Long-circulating liposomes: development and perspectives. *J. Liposome Res.* 2:321–334.

Klibanov, A. L., K. Maruyama, V. P. Torchilin, and L. Huang. 1990. Amphipathic polyethylene glycols effectively prolong the circulation time of liposomes. *FEBS Lett.* 268:235–237.

Kuhl, T. L., D. E. Leckband, D. D. Lasic, and J. N. Israelachvili. 1994. Modulation of interaction forces between bilayers exposing short-chained ethylene oxide headgroups. *Biophys. J.* 66:1479–1488.

Lasic, D. D., F. J. Martin, A. Gabizon, S. K. Huang, and D. Papahadjopoulos. 1991a. Sterically stabilized liposomes: a hypothesis on the molecular origin of the extended circulation times. *Biochim. Biophys. Acta.* 1070:187–192.

Lasic, D. D., M. C. Woodle, F. J. Martin, and T. Valentincic. 1991b. Phase behavior of "stealth-lipid"-lecithin mixtures. *Period. Biol.* 93:287–290.

Lee, J. H., J. Kopecek, and J. D. Andrade. 1989. Protein-resistant surfaces prepared by PEO-containing block copolymer surfactants. *J. Biomed. Mater. Res.* 23:351–368.

LeNeveu, D. M., R. P. Rand, V. A. Parsegian, and D. Gingell. 1977. Measurement and modification of forces between lecithin bilayers. *Biophys. J.* 18:209–230.

Lesslauer, W., J. E. Cain, and J. K. Blasie. 1972. x-ray diffraction studies of lecithin bimolecular leaflets with incorporated fluorescent probes. *Proc. Nat. Acad. Sci. USA.* 69:1499–1503.

Luckham, P. F., and J. Klein. 1985. Interactions between smooth solid surfaces in solutions of adsorbing and non-adsorbing polymers in good solvent conditions. *Macromolecules.* 18:721–728.

Mabrey, S., and J. M. Sturtevant. 1976. Investigation of phase transitions of lipids and lipid mixtures by high-sensitivity differential scanning calorimetry. *Proc. Nat. Acad. Sci. USA.* 73:3862–3866.

Marra, J., and M. L. Hair. 1988. Surface forces between two layers of poly(ethyleneoxide) adsorbed from toluene on mica. *J. Colloid Interface Sci.* 125:552–560.

Mason, J. T., C.-H. Huang, and R. L. Biltonen. 1981. Calorimetric investigations of saturated mixed-chain phosphatidylcholine bilayer dispersions. *Biochemistry.* 20:6086–6092.

Mayhew, E. G., D. Lasic, S. Babbar, and F. J. Martin. 1992. Pharmacokinetics and antitumor activity of epirubicin encapsulated in long-circulating liposomes incorporating a polyethylene glycol-derivatized phospholipid. *Int. J. Cancer.* 51:302–309.

McDaniel, R. V., and T. J. McIntosh. 1986. x-ray diffraction studies of the cholera toxin receptor, GM1. *Biophys. J.* 49:94–96.

McDaniel, R. V., T. J. McIntosh, and S. A. Simon. 1983. Non-electrolyte substitution for water in lecithin bilayers. *Biochim. Biophys. Acta.* 731: 97–108.

McIntosh, T. J. 1980. Differences in hydrocarbon chain tilt between hydrated phosphatidylethanolamine and phosphatidylcholine bilayers: a molecular packing model. *Biophys. J.* 29:237–246.

McIntosh, T. J., and P. W. Holloway. 1987. Determination of the depth of bromine atoms in bilayers formed from bromolipid probes. *Biochemistry.* 26:1783–1788.

McIntosh, T. J., A. D. Magid, and S. A. Simon. 1987. Steric repulsion between phosphatidylcholine bilayers. *Biochemistry.* 26:7325–7332.

McIntosh, T. J., A. D. Magid, and S. A. Simon. 1989a. Cholesterol modifies the short-range repulsive interactions between phosphatidylcholine membranes. *Biochemistry.* 28:17–25.

McIntosh, T. J., A. D. Magid, and S. A. Simon. 1989b. Range of the solvation pressure between lipid membranes: dependence on the packing density of solvent molecules. *Biochemistry.* 28:7904–7912.

McIntosh, T. J., R. V. McDaniel, and S. A. Simon. 1983. Induction of an interdigitated gel phase in fully hydrated lecithin bilayers. *Biochim. Biophys. Acta.* 731:109–114.

McIntosh, T. J., and S. A. Simon. 1986. The hydration force and bilayer deformation: a reevaluation. *Biochemistry.* 25:4058–4066.

McIntosh, T. J., S. A. Simon, D. Needham, and C.-H. Huang. 1992. Interbilayer interactions between sphingomyelin and sphingomyelin:cholesterol bilayers. *Biochemistry.* 31:2020–2024.

Milner, S. T. 1988. Compressing polymer brushes: a quantitative comparison of theory and experiment. *Europhys. Lett.* 7:695–699.

Milner, S. T. 1991. Polymer brushes. *Science.* 251:905–914.

Milner, S. T., T. A. Witten, and M. E. Cates. 1988. Theory of the grafted polymer brush. *Macromolecules.* 21:2610–2619.

Mori, A., A. L. Klibanov, V. P. Torchilin, and L. Huang. 1991. Influence of the steric barrier activity of amphipathic poly(ethyleneglycol) and ganglioside GM1 on the circulation time of liposomes and on the target binding of immunoliposomes in vivo. *FEBS Lett.* 284:263–266.

Napper, D. H. 1983. Polymeric Stability of Colloidal Dispersions. Academic Press, New York.

Needham, D., K. Hristova, T. J. McIntosh, M. Dewhirst, N. Wu, and D. D. Lasic. 1992. Polymer-grafted liposomes: physical basis for the "stealth" property. *J. Liposome Res.* 2:411–430.

Needham, D., and T. J. McIntosh. 1991. Mechanical and interactive properties of lipid membranes containing surface-bound polymer: implications for liposome delivery design. *Biophys. J.* 59:500*a* (Abstr.).

Needham, D., T. J. McIntosh, and D. D. Lasic. 1992. Repulsive interactions and mechanical stability of polymer-grafted lipid membranes. *Biochim. Biophys. Acta.* 1108:40–48.

Papahadjopoulos, D., T. M. Allen, A. Gabizon, E. Mayhew, K. Matthay, S. K. Huang, K.-D. Lee, M. C. Woodle, D. D. Lasic, C. Redemann, and F. J. Martin. 1991. Sterically stabilized liposomes: improvements in pharmacokinetics and antitumor therapeutic efficacy. *Proc. Nat. Acad. Sci. USA.* 88:11460–11464.

Parsegian, V. A., R. P. Rand, N. L. Fuller, and R. C. Rau. 1986. Osmotic stress for the direct measurement of intermolecular forces. *Methods Enzymol.* 127:400–416.

Patel, S., and M. Tirrell. 1989. Measurement of forces between surfaces in polymer fluids. *Annu. Rev. Phys. Chem.* 40:597–635.

Patel, S., M. Tirrell, and G. Hadziioannou. 1988. A simple model for forces between surfaces bearing grafted polymers applied to data on adsorbed block copolymers. *Colloids Surf.* 31:157–179.

Pearson, R. H., and I. Pascher. 1979. The molecular structure of lecithin dihydrate. *Nature.* 281:499–501.

Ranck, J. L., T. Keira, and V. Luzzati. 1977. A novel packing of the hydrocarbon chains in lipids. The low temperature phase of DPPG. *Biochim. Biophys. Acta.* 488:432–441.

Ribeiro, A. A., and E. A. Dennis. 1975. Proton magnetic resonance relaxation studies on the structure of mixed micelles of Triton X-100 and dimyristoylphosphatidylcholine. *Biochemistry.* 14:3746–3755.

Ribeiro, A. A., and E. A. Dennis. 1987. Structure and dynamics by NMR and other methods. *In* Nonionic Surfactants: Physical Chemistry. M. J. Schick, editor. Marcel Dekker, New York. 971–1009.

Rowe, E. S. 1987. Induction of lateral phase separations in binary lipid mixtures by alcohol. *Biochemistry.* 26:46–51.

Sarmoria, C., and D. Blankschtein. 1992. Conformation characteristics of short poly(ethylene oxide) chains terminally attached to a wall and free in aqueous solution. *J. Phys. Chem.* 96:1978–1983.

Sayre, D. 1952. Some implications of a theorem due to Shannon. *Acta Crystallogr. Sect. B. Struct. Crystallogr. Cryst. Chem.* 5:843.

Shannon, C. E. 1949. Communication in the presence of noise. *Proc. Inst. Radio Engrs. N. Y.* 37:10–21.

Simon, S. A., and T. J. McIntosh. 1984. Interdigitated hydrocarbon chain packing causes the biphasic transition behavior in lipid/alcohol suspensions. *Biochim. Biophys. Acta.* 773:169–172.

Simon, S. A., T. J. McIntosh, and M. L. Hines. 1986. The influence of anesthetics on the structure and thermal properties of saturated lecithins. *In* Molecular and Cellular Mechanisms of Anesthetics. S. H. Roth and K. Miller, editors. Plenum Publishing Co. New York, 297–308.

Simon, S. A., T. J. McIntosh, and R. Latorre. 1982. Influence of cholesterol on water penetration into bilayers. *Science.* 216:65–67.

Sparling, M. L., R. Zidovetzki, L. Muller, and S. I. Chan. 1989. Analysis of membrane lipids by 500 MHz ^{1}H NMR. *Anal. Biochem.* 178:67–76.

Swamy, M. J., B. Angerstein, and D. Marsh. 1994. Differential scanning calorimetry of thermotropic phase transitions in vitaminylated lipids: aqueous dispersions of *N*-biotinyl phosphatidylethanolamines. *Biophys. J.* 66:31–39.

Tardieu, A., V. Luzzati, and F. C. Reman. 1973. Structure and polymorphism of the hydrocarbon chains of lipids: a study of lecithin-water phases. *J. Mol. Biol.* 75:711–733.

Taunton, H. J., C. Toprakcioglu, L. J. Fetters, and J. Klein. 1990. Interactions between surfaces bearing end-adsorbed chains in a good solvent. *Macromolecules.* 23:571–580.

Tirrell, M., S. Patel, and G. Hadziioannou. 1987. Polymeric amphiphiles at solid-fluid interfaces: forces between layers of adsorbed block copolymers. *Proc. Nat. Acad. Sci. USA.* 84:4725–4728.

Torchilin, V. P., A. L. Klibanov, L. Huang, S. O'Donnell, N. D. Nossiff, and B. A. Khaw. 1992. Targeted accumulation of polyethylene glycol-coated immunoliposomes in farcted rabbit myocardium. *FASEB J.* 6:2716–2719.

Tristram-Nagle, S., R. M. Suter, W.-J. Sun, and J. F. Nagle. 1994. Kinetics of subgel formation in DPPC: x-ray diffraction proves nucleation-growth hypothesis. *Biochim. Biophys. Acta.* 1191:14–20.

Vaage, J., D. Donovan, E. Mayhew, P. Uster, and M. Woodle. 1993. Therapy of mouse mammary carcinomas with vincristine and doxorubicin encapsulated in sterically stabilized liposomes. *Int. J. Cancer.* 54:959–964.

Walter, A., P. K. Vinson, A. Kaplun, and Y. Talmon. 1991. Intermediate structures in the cholate-phosphatidylcholine vesicle-micelle transition. *Biophys. J.* 60:1315–1325.

Wiener, M. C., R. M. Suter, and J. F. Nagle. 1989. Structure of the fully hydrated gel phase of dipalmitoylphosphatidylcholine. *Biophys. J.* 55: 315–325.

Williams, S. S., T. R. Alosco, E. Mayhew, D. D. Lasic, F. J. Martin, and R. B. Bankert. 1993. Arrest of human lung tumor xenograft growth in severe combined immunodeficient mice using doxorubicin encapsulated in sterically stabilized liposomes. *Cancer Res.* 53:3964–3967.

Woodle, M. C., and D. D. Lasic. 1992. Sterically stabilized liposomes. *Biochim. Biophys. Acta.* 1113:171–199.

Woodle, M. C., K. K. Matthay, M. S. Newman, J. E. Hidayat, L. R. Collins, C. Redemann, F. J. Martin, and D. Papahadjopoulos. 1992. Versatility in lipid compositions showing prolonged circulation with sterically stabilized liposomes. *Biochim. Biophys. Acta.* 1105:193–200.

Worcester, D. L., and N. P. Franks. 1976. Structural analysis of hydrated egg lecithin and cholesterol bilayers II. Neutron diffraction. *J. Mol. Biol.* 100:359–378.

Worthington, C. R. 1969. The interpretation of low-angle x-ray data from planar and concentric multilayered structures. The use of one-dimensional electron density strip models. *Biophys. J.* 9:222–234.

Worthington, C. R., G. I. King, and T. J. McIntosh. 1973. Direct structure determination of multilayered membrane-type systems which contain fluid layers. *Biophys. J.* 13:480–494.

Wu, N. Z., D. Da, T. L. Rudoll, D. Needham, and M. W. Dewhirst. 1993. Increased microvascular permeability contributes to preferential accumulation of stealth liposomes in tumor tissue. *Cancer Res.* 53:3765–3770.